SOLID LUBRICATION OF LASER GROWN FLUORINATED DIAMOND THIN FILMS

Final Report for SBIR, Phase I Research
July 1, 1991 through December 31, 1991

Contract No. DAAL 03-91-C-0041

Prepared for:

Strategic Defense Initiative Organization

Monitored by:

U.S. Army Research Office
P.O. Box 12211
Research Triangle Park
North Carolina 27709-2211

LASER SCIENCE COMPANY
ISIS Center, Suite 603
2501 North Loop Drive
Ames, IA 50010-8283

REPORT DOCUMENTATION PAGE

Form Approved
OMB No. 0704-0188

1. AGENCY USE ONLY (Leave blank)	2. REPORT DATE	3. REPORT TYPE AND DATES COVERED
	Jan. 21, 1992	Final Report, July 1 - Dec. 31, 1991

4. TITLE AND SUBTITLE
SOLID LUBRICATION OF LASER GROWN FLUORINATED DIAMOND FILMS

5. FUNDING NUMBERS
DAAL03-91-C-0041

6. AUTHOR(S)
Bruce Janvrin, Madhav Rao, Deli Gong,
Arul Molian, P. Molian

7. PERFORMING ORGANIZATION NAME(S) AND ADDRESS(ES)
Laser Science Company
ISIS Center, #603, ISU Research Park
2501 North Loop Drive
Ames, IA 50010-8283

8. PERFORMING ORGANIZATION REPORT NUMBER

9. SPONSORING/MONITORING AGENCY NAME(S) AND ADDRESS(ES)
U. S. Army Research Office
P. O. Box 12211
Research Triangle Park, NC 27709-2211

10. SPONSORING/MONITORING AGENCY REPORT NUMBER
ARO 29043.1-MS-SBI

11. SUPPLEMENTARY NOTES
The view, opinions and/or findings contained in this report are those of the author(s) and should not be construed as an official Department of the Army position, policy, or decision, unless so designated by other documentation.

12a. DISTRIBUTION/AVAILABILITY STATEMENT
Approved for public release; distribution unlimited.

12b. DISTRIBUTION CODE

13. ABSTRACT *(Maximum 200 words)*

A laser chemical vapor deposition process has been developed to grow fluorinated diamond thin films on bearing material substrates including SiC and 440C stainless steel. The type of laser, carbon feedstock, laser-precursor gas interactions, and deposition conditions have been established. Analysis of laser grown films revealed that the films deposited on SiC consisted of a mixture of diamond and graphite while the films on 440C steel were composed of diamond, diamond-like carbon and graphite. The presence of significant amount of C-F compounds both in the surface and subsurface layers was also identified. Tribological tests (ball-on-disc and pin-on-disc) of laser grown films under ambient environment indicated a friction coefficient in the range of 0.1 to 0.3 depending on the wear couple, sliding speed and load confirming the effectiveness of these films as solid lubricants for moving mechanical assemblies in space structures. Fluorination of carbon films has attributes: passivation of the surface of diamond/graphite films from absorption of water or oxygen, reduction of surface energy needed for shearing of the film during solid lubrication, and protection from corrosive environments.

14. SUBJECT TERMS	15. NUMBER OF PAGES
Diamond, Thin Films, Lasers, Fluorination, Solid Lubrication	58
	16. PRICE CODE

17. SECURITY CLASSIFICATION OF REPORT	18. SECURITY CLASSIFICATION OF THIS PAGE	19. SECURITY CLASSIFICATION OF ABSTRACT	20. LIMITATION OF ABSTRACT
UNCLASSIFIED	UNCLASSIFIED	UNCLASSIFIED	UL

GENERAL INSTRUCTIONS FOR COMPLETING SF 298

The Report Documentation Page (RDP) is used in announcing and cataloging reports. It is important that this information be consistent with the rest of the report, particularly the cover and title page. Instructions for filling in each block of the form follow. It is important to ***stay within the lines*** to meet ***optical scanning requirements***.

Block 1. Agency Use Only *(Leave blank)*.

Block 2. Report Date. Full publication date including day, month, and year, if available (e.g. 1 Jan 88). Must cite at least the year.

Block 3. Type of Report and Dates Covered. State whether report is interim, final, etc. If applicable, enter inclusive report dates (e.g. 10 Jun 87 - 30 Jun 88).

Block 4. Title and Subtitle. A title is taken from the part of the report that provides the most meaningful and complete information. When a report is prepared in more than one volume, repeat the primary title, add volume number, and include subtitle for the specific volume. On classified documents enter the title classification in parentheses.

Block 5. Funding Numbers. To include contract and grant numbers; may include program element number(s), project number(s), task number(s), and work unit number(s). Use the following labels:

C	- Contract	**PR**	- Project
G	- Grant	**TA**	- Task
PE	- Program Element	**WU**	- Work Unit Accession No.

Block 6. Author(s). Name(s) of person(s) responsible for writing the report, performing the research, or credited with the content of the report. If editor or compiler, this should follow the name(s).

Block 7. Performing Organization Name(s) and Address(es). Self-explanatory.

Block 8. Performing Organization Report Number. Enter the unique alphanumeric report number(s) assigned by the organization performing the report.

Block 9. Sponsoring/Monitoring Agency Name(s) and Address(es). Self-explanatory.

Block 10. Sponsoring/Monitoring Agency Report Number. *(If known)*

Block 11. Supplementary Notes. Enter information not included elsewhere such as: Prepared in cooperation with...; Trans. of...; To be published in.... When a report is revised, include a statement whether the new report supersedes or supplements the older report.

Block 12a. Distribution/Availability Statement. Denotes public availability or limitations. Cite any availability to the public. Enter additional limitations or special markings in all capitals (e.g. NOFORN, REL, ITAR).

- **DOD** - See DoDD 5230.24, "Distribution Statements on Technical Documents."
- **DOE** - See authorities.
- **NASA** - See Handbook NHB 2200.2.
- **NTIS** - Leave blank.

Block 12b. Distribution Code.

- **DOD** - Leave blank.
- **DOE** - Enter DOE distribution categories from the Standard Distribution for Unclassified Scientific and Technical Reports.
- **NASA** - Leave blank.
- **NTIS** - Leave blank.

Block 13. Abstract. Include a brief *(Maximum 200 words)* factual summary of the most significant information contained in the report.

Block 14. Subject Terms. Keywords or phrases identifying major subjects in the report.

Block 15. Number of Pages. Enter the total number of pages.

Block 16. Price Code. Enter appropriate price code *(NTIS only)*.

Blocks 17. - 19. Security Classifications. Self-explanatory. Enter U.S. Security Classification in accordance with U.S. Security Regulations (i.e., UNCLASSIFIED). If form contains classified information, stamp classification on the top and bottom of the page.

Block 20. Limitation of Abstract. This block must be completed to assign a limitation to the abstract. Enter either UL (unlimited) or SAR (same as report). An entry in this block is necessary if the abstract is to be limited. If blank, the abstract is assumed to be unlimited.

TABLE OF CONTENTS

	PAGE
REPORT DOCUMENTATION PAGE	i
ACKNOWLDGEMENTS	ii
LIST OF TABLES	iii
LIST OF FIGURES	iv
1. INTRODUCTION	1
2. TECHNICAL OBJECTIVES AND FEASIBILITY	4
3. EXPERIMENTAL DETAILS	7
4. RESULTS AND DISCUSSION	10
5. ESTIMATES OF PHASE I TECHNICAL FEASIBILITY	21
6. POTENTIAL FOR DoD	22
7. CONCLUSION	23
8. REFERENCES	24
FIGURES	26

ACKNOWLEDGEMENTS

This SBIR Phase I research program was sponsored by Strategic Defense Initiative Organization and was monitored by U.S. Army Research Office. Their support, encouragement and useful discussions with Contract Technical Monitor Dr. Robert Reeber are gratefully acknowledged. We are deeply grateful to Iowa State University for technical collaboration.

LIST OF TABLES

Table		Page
1	Properties of CVD diamond films	2
2	Literature data on laser CVD growth of diamond	3
3	Laser-precursor gas interactions	5
4	Photochemistry of precursor gases	6
5	Specifications of laser systems used	8
6	Nd:YAG laser CVD experiments	10
7	Excimer laser CVD experiments for SiC substrate	13
8	XPS analysis of laser grown films	16
9	Excimer laser CVD experiments for 440C steel substrate	17
10	Friction of laser grown films on SiC substrate	19
11	Friction of laser grown films on 440C steel substrate	19

LIST OF FIGURES

Figure		Page
1	Laser CVD interaction processes during perpendicular irradiation of laser beam on the substrate surface	26
2	Schematic diagram showing laser CVD experimental set-up. A single laser beam (YAG or Excimer) was only used for each experiment	27
3	Photographs of laser CVD experiment. A: Excimer laser B: Nd:YAG laser, C: Vacuum chamber	28
4	Reference Raman spectra for diamond, graphite and diamond-like carbon	29
5	Schematic of ball-on-disc tribotest rig	30
6	Scanning electron micrographs of 248-nm KrF beam processed SiC (Hexaloy grade)	31
7	Scanning electron micrographs of Sample # 55 showing a mixture of fluorinated diamond and graphite on SiC substrate	33
8	Raman spectrum of Sample # 55 showing the peaks for diamond and graphite. Note the absence of SiC peaks at 786 cm^{-1} and 965 cm^{-1}.	34
9	Scanning electron micrographs of diamond films (a) Laser grown film on SiC (b) Hot filament CVD grown film on Si	35
10	Scanning electron micrographs of laser grown films on SiC substrate (a) 193-nm ArF beam processed (b) 248-nm KrF beam processed	36
11	Scanning electron micrographs of laser grown films on SiC (a) Without gas preheating (b) With gas preheating	37
12	Raman spectrum of Sample # 57 showing diamond and DLC peaks in addition to SiC peaks	38
13	Raman spectrum of Sample # 58 showing diamond and DLC peaks in addition to SiC peaks	39
14	Raman spectrum of Sample # 64 showing diamond and DLC peaks Note the absence of SiC peaks	40

Figure		Page
15	Raman spectrum of Sample # 65 showing diamond and DLC peaks Note the absence of SiC peaks	41
16	Raman spectrum of Sample # 73 showing diamond and DLC peaks in addition to SiC peaks	42
17	Raman spectrum of hot-filament CVD grown diamond film on Si	43
18	Wavelength dispersive X-ray spectrum of Sample # 74 showing carbon and fluorine	44
19	Full scale XPS spectrum of SiC substrate	45
20	Full scale XPS spectrum of Sample # 64	46
21	Full scale XPS spectrum of Sample # 74	47
22	Scanning electron micrograph of laser grown film on 440C stainless steel. The dark zone is a beam-masked area intended to determine the thickness of film	48
23	Scanning electron micrographs of Sample # 35 showing ball-like diamond structures	49
24	Scanning electron micrographs of Sample # 50 showing mixed carbon structures	50
25	Raman spectrum of Sample # 35 showing diamond and DLC	51
26	Raman spectrum of Sample # 38 showing diamond and graphite	52
27	Raman spectrum of Sample # 40 showing DLC and graphite	53
28	Raman spectrum of Sample # 46 showing diamond, DLC and graphite	54
29	Raman spectrum of Sample # 50 showing DLC and graphite	55
30	Effect of beam wavelength on Raman spectrum of diamond films (a) 193-nm ArF beam processed (b) 248-nm KrF beam processed	56
31	Friction data for three commonly employed space lubricants (After Reference 6)	57
32	Friction of diamond/graphite films on 440C steel (a) Source: Reference 7 (b) Source: Reference 8	58

1. INTRODUCTION

Numerous space tribosystem components (turbine mainshaft bearings, missile main shaft bearings, pointing control MMAs bearings, transmission gears, gimbal bearings, caged bearings, airframe bearings, and supersonic aircraft engines including adiabatic diesel, small gas turbine, and rotary engines) require solid lubricants to resist extreme environments including: variable temperature, radiation exposure, and a variety of atmospheres from ultra-high vacuum to highly oxidizing or corrosive environment [1,2]. Liquid lubricants could not be applied for the space environments because of their volatility due to high vapor pressure, and degradation due to temperature variation and atomic oxygen environment. Solid lubricants offer the following benefits:

- o good stability at extreme temperatures and in chemically reactive environments
- o high load-carrying capacity
- o bearings can be placed closer to the heat sources allowing the use of short shafts
- o resistant to radiation, and
- o light weight structures.

The limitations of solid lubricants include higher friction coefficient than obtainable with hydrodynamic lubrication, wear due to solid-solid contact, inadequate cooling capacity and replenishment. MoS_2, WS_2, graphite, plastics, soft metal films, oxides, sulfides, fluorides and nitrides are commonly used as solid lubricants. The friction coefficient varies from 0.05 to 0.2 depending upon temperature, environment, load, speed and presence of foreign material. Todate, ultra-low coefficients of friction (0.02), extremely low wear, and long endurance lives have been obtained for sputtered MoS_2 films [3,4].

A solid lubricant, in order to function effectively, should fulfill the following requirements:

1. Low shear strength -- allows shear to occur at the sliding interface
2. High wear resistance -- withstands fracture and defect growth in the film
3. High adhesive strength -- prevents peeling off from the substrate surface
4. High thermal conductivity -- dissipates the heat generated

The solid lubricants specified above meet fully the first criteria but partially the others. Several new solid lubricants involving polymers, glasses and inorganic compounds are being researched for space structures. In Phase I work, we have developed laser grown fluorinated diamond film as a solid lubricant because it has the potential to satisfy all the four criteria. Fluorinated carbon exhibits low surface energy and gives rise to excellent shearing. Diamond is the superhard material and can provide the highest wear resistance. Diamond, being 4 to 5 times higher than copper in thermal conductivity, can also provide the heat dissipation capability. Strong adhesion of the film is promoted by the laser processing and by the proper selection of substrate material.

The technologically attractive properties of diamond films are given in Table 1. Friction and wear studies of CVD diamond and DLC films have indicated a friction coefficient on the order of 0.2 or less [5-9]. The friction coefficient is even reduced to 0.01-0.02 at low humidity (1% RH) but increased to 0.2 or higher at 100% RH. Low friction is mostly due to the presence of hydrogen. However, vacuum environment increases the friction by desorpting hydrogen from the film. Between diamond and DLC films, the latter was better due to smooth surfaces and strong adherence to the substrate.

Table 1. Properties of Diamond Films

High thermal conductivity
High hole mobility, dopability
Wide bandgap, low dielectric constant
Optical transparency (> 230 nm)
Low thermal expansion
Low friction
Superior wear resistance
Very high hardness
Chemical inertness
High sound propagation velocity
Biocompatibility

Diamond thin films are produced by a variety of chemical vapor deposition (CVD) procedures including plasma, microwave, hot-filament, ion beam, and electron beam. Numerous papers dealing with CVD diamond synthesis have appeared in recent years [10]. Most of the CVD processes suffer from: low deposition rate and area coverage, high substrate temperature, presence of hydrogen and graphite impurities, poor adhesion and rough surface. New methods are needed for fabrication of diamond thin films to overcome some limitations of existing methods and possibly improve the quality of diamond films. One such method is laser-induced CVD (LCVD) where a laser beam serves as an energy source for decomposing the gases and to raise the surface temperature of the substrate for deposition. Laser technology for diamond film fabrication is very new and todate only a handful number of publications are available that address directly on the CVD diamond growth. Lasers are capable of providing the economical and technical benefits through reduced fabrication time and better quality over the existing diamond CVD technology. Some of the unique features of LCVD are: clean source of energy, possibility of obtaining high deposition rate, low substrate temperature, selective area deposition, and better surface integrity.

A literature review of laser-induced CVD for diamond deposition indicates that limited work has been carried out. Most of the reported work involved the use of an excimer laser beam for photochemical decomposition of organic gas molecules. The beam was incident either normal or parallel to the substrate surface. A summary of data available on LCVD for diamond growth is given in Table 2.

Table 2. Literature Data on Laser CVD Growth of Diamond

Reference	Experimental Details	Remarks
Goto et al [11]	ArF-Excimer laser using CCl_4 and 450°C substrate temp.	Atomic hydrogen is needed 1-3 microns/hour
Tyndall and Hacker [12]	KrF-Excimer using CH_3COOH and 20°C substrate temperature	Neither diamond seed nor atomic hydrogen needed
Celii et al [13]	ArF-Excimer laser assisted hot filament technique	Diamond is suppressed
Janvrin and Molian [14]	ArF-Excimer laser using organic precursors	Atomic hydrogen is needed Low substrate temp. 200°C
Molian et al [15]	CO_2 laser using CH_4/H_2	Good quality diamond
Thaler [16]	CO_2 laser using SF_6/CH_4	Hydrogen-free, Amorphous diamond
Chapliev et al [17]	KrF-excimer assisted plasma CVD	Selective area deposition

The chief advantage of laser CVD is the low temperature deposition. For excimer laser-induced CVD, CH_4 is not used as a precursor because it does not absorb the excimer wavelength. ArF (193 nm) excimer beam is not appropriate especially for perpendicular radiation because diamond transmits the light only at a wavelength greater than 225 nm. Recently, a different laser method beginning with carbon ion implantation followed by pulsed excimer laser melting was developed to produce defect-free, single crystalline diamond films on a copper substrate [18].

A recent development in diamond thin films has been the fluorination of diamond which has been suggested as a means of reducing the coefficients of friction of diamond surfaces when adsorbed water or oxygen is present [5,19]. Fluorine atoms can provide the passivation of surface resisting the diffusion of oxygen. This factor is very significant in space applications where atomic oxygen is present. In Phase I research, we have developed a laser CVD growth technique for producing fluorinated diamond films and determined the tribological characteristics of such films for space applications.

2. TECHNICAL OBJECTIVES AND FEASIBILITY

2.1 Objectives

The technical objectives of Phase I research are:

1. to develop a laser CVD technique for growing fluorinated diamond films on SiC and 440C steel substrates using halogenated methane precursors

2. to characterize the films with scanning electron microscope, Raman spectroscope and X-ray photoelectron spectroscope

3. to determine tribological characteristics of the films and compare with presently employed space lubricants

2.2 Parallel and Normal Irradiation

In laser CVD, the nucleation and growth mechanisms are dependent on the method of laser irradiation namely normal incidence or parallel incidence to the substrate or both using a dual beam approach. In parallel incidence, lasers can induce chemical reactions homogeneously within the gas phase and reaction products are diffusion driven towards the substrate surface giving rise to thin films. There is no damage to the substrate by this process. In normal incidence, the laser beam causes heterogeneous reactions to occur at the gas-solid interface. Such reactions facilitate the vapor-solid condensation on the surface. It should be stressed that solid surfaces are potential sites for decomposing the gaseous molecules. Depending upon the energy density of laser beam, various other processes can also take place including etching, melting and vaporization. The interactions between the laser beam and the substrate in the presence of a gaseous environment during perpendicular radiation are summarized in Figure 1. Laser energy density should be reduced in order to prevent the damage to the thin film by etching, melting and vaporization. The best approach is to find the optimum energy density required for decomposition of gases, and heating of the substrate to just below melting temperature.

In Phase I research, we have found that homogeneous reactions by parallel laser irradiation of the precursor gas volume did not lead to any deposition. Hence experiments and results are reported only on the normal incidence. Angular incidence of the beam can also be used but reflection energy losses are much higher than normal incidence.

2.3 Lasers and Precursors

Lasers can decompose gaseous molecules by pyrolysis and photolysis mechanisms. In laser pyrolysis, the gases are excited by the beam irradiation, and the substrate is heated to the desired temperature by controlling the power and irradiation time of the beam, while the excited gases decompose by collisional excitation with the hot surface. The laser-driven reactions are significantly different from other CVD sources for a given heat input because the focused beam produces higher temperatures in a smaller volume [20]. In laser photolysis process, the photons break the chemical bonds of the gaseous

molecules and allows the products get deposited on the substrate. An important requirement in photolysis is that the gases should absorb the laser radiation. In general, pyrolysis is more efficient than photolysis. In Phase I work, we have used both approaches to synthesize diamond films. A summary of lasers and precursors used is given in Table 3.

2.4 Feasibility of Nd:YAG Laser Pyrolytic CVD for Diamond Growth

The origin for using laser pyrolytic CVD using Nd:YAG laser to synthesize diamond was based upon Rudder et al's [21] work on thermal CVD of CF_4/F_2. Mass spectrometric analysis of thermal CVD of CF_4/F_2 revealed the presence of F, F_2 and CF_x radicals [21]. Rudder et al concluded that atomic fluorine behaves similar to hydrogen namely that it etches away the nondiamond phases. The laser energy absorbed by the precursor gas mixture (CF_4/F_2 or CCl_4/F_2) cause them to be in the excited, high-energy state. When the excited gases come in contact with the hot substrate, adsorption of gaseous layer occurs on the substrate surface followed by a reaction to form adsorbed layers of atomic fluorine. The adsorbed fluorine atoms then form clusters which grow and coalesce to form a continuous film. Once a nanolayer of atomic fluorine is formed, nucleation of carbon takes place as a result of decomposition of CF_4 or CCl_4 organic precursor. The free carbon atoms form clusters and provide nucleation centers for further film growth. Although the carbon can be deposited as diamond or graphite or other forms of carbon such as chaoite, lonsdaleite and carbyne, the probability of diamond deposition is more likely because the atomic fluorine etches away other forms of carbon.

Table 3. Laser-Precursor Gas Interactions

Lasers	
Nd:YAG	-- 1064 nm wavelength, provide thermal mechanisms, photolytic effects are none or minimal
Excimer	-- 193-351 nm wavelength, provide photolytic as well as pyrolytic mechanisms
Precursor Gases	
CF_4	-- Can not be photolytically decomposed with excimer lasers -- Can be thermally decomposed to C-F species at 1500°C
F_2	-- Can be photolytically decomposed by wavelengths less than 400 nm -- Can also be thermally cracked at 1500°C
CCl_4	-- Can be photolytically decomposed at wavelength less than 250 nm -- Can be thermally dissociated at 600°C

If we assume that halogenated methane behaves similar to CH_4, then sp^3 configuration can be enhanced by CF_3 and CF radicals while the graphite is formed by the CF_2 and C_2 radicals. The CF_3 radical is the desired species for

growing the diamond cubic structure. Infrared lasers such as Nd:YAG decompose pyrolytically CF_4 molecules to excited radicals of CF_3 by thermally dissociating the gases at the hot substrate surface ($> 900^0C$). Once sp^3 orbitals of CF_3 are formed, methods must be taken to stabilize the sp^3 bonding. Atomic fluorine, similar to atomic hydrogen, can assist in binding the metastable sp^3 structures as well as passivates the surface dangling bonds. Atomic fluorine is produced from two sources: decomposition of CF_4 and dissociation of F_2 at temperatures greater than 900^0C. The stabilization of sp^3 and its bonding to the substrate are also dependent upon the energy of ions or electrons or other species that impact the growing film. Laser assistance is expected to enhance surface binding.

2.5 Feasibility of Excimer Laser Photolytic CVD for Diamond Growth

In laser photochemical reactions, the gaseous precursor must absorb the photons directly and that the photon energy must be larger than the binding energy of the gases. CCl_4 and F_2 used as precursor gases in this study can be dissociated by the laser wavelengths 193 nm and 248 nm. Table 4 gives the supporting data [22]. The dissociation of F_2 into atomic species is accompanied by a heat release of 37 Kcal/mole. CF_4 is photolytically stable and can be thermally cracked at temperatures 1500^0C or more while CCl_4 can be photolytically dissociated as well as thermally at 600^0C. The absorption wavelength for CF_4 is 160 nm and the bond energy for C-F is 120 Kcal which is much higher than that of the photon energy of KrF-beam (114 Kcal).

A previous study indicated the possibility of obtaining diamond films with CCl_4/H_2 gas mixture in excimer laser CVD if atomic hydrogen is made available. It is envisioned that F_2 molecules decomposed to the small size F atoms (photolytically) will provide the capabilities for etching nondiamond phases.

Table 4. Photochemistry of Precursor Gases

Gas	Binding energy	Absorption wavelength	Dissociation
F_2	1.5 eV	< 400 nm	F_2 ----> 2 F
CCl_4	3.0 eV	< 250 nm	CCl_4 ----> CCl+ Cl_2+Cl

3. EXPERIMENTAL DETAILS

3.1 Substrates

Since the application of this project is focused on space bearings, two bearing materials namely SiC (alpha) and 440C stainless steel were selected as substrates. Two different substrates were chosen to explore the potential of substrate and its surface as a catalyst site to facilitate the laser/gas/surface reactions on diamond film growth and morphology. No scratching and seeding the surface with diamond powders was done to increase the nucleation rate because laser beam in normal radiation mode can "clean" such seeding.

SiC is an excellent substrate for diamond growth due to lattice matching. It is also the material for next-generation space bearings because of the following reasons: SiC bearings are about 50% of the weight of steel bearings; SiC has higher elastic modulus and hence can be designed for higher preload (reduces torque or friction because of higher preload); SiC can be made to geometric precision, has excellent chemical resistance and has increased life for precision MMAs and actuator designs.

Three different sources of SiC were experimented. These include:

Carborundum, Hexaloy Grade SA
Norton, NC 203
ESK Engineered Ceramics, EKasic HD

The SiC substrates obtained from Carborundum and Norton were sintered alpha (hexagonal) and contained some impurities. EKasic grade is a high purity SIC (99.5%) and was produced by hot isostatic pressing (HIP). The steel substrates were obtained as flat specimens as well as in the form of ball bearings.

3.2 Selection of Precursor

Traditionally, CH_4 diluted in hydrogen is employed as a precursor by most CVD methods. In LCVD, CH_4 is not a suitable gas because the decomposition of CH_4 can occur only with wavelengths of light less than 160 nm [22]. The precursor gases used were CCl_4, 1% CF_4/1% F_2/98% He (designated as X hereafter) and CCl_2F_2 mixed with and without hydrogen. X was obtained from Air Products Ltd.

It has previously been demonstrated by many researchers that the addition of a small amount of oxygen to the precursor gases can reduce the graphite formation and can also increase diamond deposition rate. This is explained to be due to the production of atomic hydrogen by chemical reactions to form H and OH. In Phase I, oxygen was added to C-F-H system in some experiments.

In some experiments, the effect of preheating of the precursor gases on the diamond growth was examined. Preheating was accomplished by flowing the gases over a W-filament suspended in a quartz tube which in turn was heated by means of a small furnace upto 1000°C. But the results indicated the presence of W in the film and so the filament was replaced by a stainless tube which contained fins to activate the precursor gases.

3.3 Lasers

Two lasers, the specifications of which are given in Table 5, were used in this work.

Table 5. Specifications of Laser Systems Used

Laser type	Nd:YAG	ArF-Excimer	KrF-Excimer
Wavelength	1060 nm	193 nm	248 nm
Average Power	10 W	10 W	30 W
Pulse length	300 microsec	17 nanosec	23 nanosec
Pulse energy	1-3 J	100 mJ	300 mJ
Pulse repetition rate	1-10 Hz	1-100 Hz	1-100 Hz

3.4 Laser Chemical Synthesis

Diamond growth experiments were conducted in a chemical vapor deposition reactor (CVD). A schematic diagram of the CVD chamber and laser processing is shown in Figure 2. The six-way vacuum chamber can be evacuated to less than 10^{-7} torr by means of diffusion and mechanical pumps. This chamber has provisions for the laser beam window, heating the substrate up to 1000°C and mounting of the target. An inlet for the gas flow into the chamber is also shown in Figure 2. A lens behind each of two windows is located in order to focus the beam on the gaseous medium or on the substrate. Although Figure 2 shows a dual-beam arrangement, all the experiments were carried out only using a single beam in parallel or normal radiation of laser beam. The beam was either 1064 nm Nd:YAG for pyrolysis or 193 nm/248 nm excimer beam for photolysis. Figure 3 is a photograph of the laser CVD experiment. Over 80 experiments involving variation of laser parameters, gas flow and substrate conditions were conducted. The substrates were ultrasonically cleaned in methanol prior to and after deposition.

3.5 Analysis and Characterization

Several analytical instruments were used to identify the growth mechanisms and to analyze the diamond films. These include:

(i) Scanning electron microscope: Wavelength dispersive x-ray analysis coupled with SEM will be used to evaluate the presence of carbon, the morphology of diamond crystallites, uniformity and coverage area

(ii) Raman microprobe spectroscope: Diamond films differ from amorphous carbon, graphite, glassy carbon and other forms of carbon by their light scattering properties. Raman spectroscope is the most widely used for signature diagnosis of diamond film. In the Raman spectrum, diamond has a peak at 1332 cm^{-1}, graphite has a peak at 1580 cm^{-1} and diamond-like carbon has peaks at 1345 cm^{-1} and 1550 cm^{-1} (Figure 4).

(iii) X-ray Photoelectron Spectroscope: XPS analysis was used to identify the presence of various fluorinated carbons

3.6 Tribological Evaluation

Friction tests using a pin-on-disc or ball-on-disc arrangement were conducted to evaluate the solid lubrication behavior of fluorinated diamond films. A schematic of the friction test apparatus is shown in Figure 5. The ball or the pin was always the diamond-coated specimen while the disc was made of a hardened tool steel (R_c = 64-66) with a surface roughness of Ra = 0.065 microns. Before each test, the triboelements were cleaned in acetone. Friction measurement was performed as a function of load and speed at ambient atmosphere and controlled humidity (65% RH).

4. RESULTS AND DISCUSSION

This section describes the results obtained using Nd:YAG pyrolytic and excimer photolytic methods. An important result during this study was the absence of any film formation in the parallel radiation mode irrespective of the type of laser used. Hence all the results pertained to the normal incidence of the laser beam on the substrate surface in which heterogeneous reactions take place.

4.1 Nd:YAG Laser Pyrolytic Deposition

The pulsed Nd:YAG laser is an intense thermal source and can pyrolytically decompose the gases homogeneously within the gas phase or heterogeneously at the solid surface. We have employed a 3 J Nd:YAG laser to pyrolytically decompose the 1% CF_4/1% F_2/98% He gas mixture at the SiC substrate. About 20 experiments were carried out but none produced satisfactory results. Table 6 provides representative experiments and results.

Table 6. Nd:YAG Laser Chemical Vapor Deposition Experiments

Laser: Pulsed Nd:YAG, 1060 nm
Substrate: SiC (alpha)
Initial Vacuum: 10^{-5} torr
Irradiation: Normal to the substrate
Lens: 150 mm focal length
Spot size: 0.40 mm dia.

Sample Number	Precursor Gas Mixture	Pressure/Flow	Laser Parameters	Deposition Time	Comments
14	X*	0.6 torr 50 sccm	0.65 J/pulse 10 Hz	30 min.	Film around microholes
15	X	1.0 torr 50 sccm	3.0 J/pulse 1 Hz	30 min.	Film around microholes
16	X + H_2	1.0 torr 50 sccm each	3.0 J/pulse 1 Hz	30 min.	Film around microholes
17	Freon R-11	1.0 torr 500 sccm	3.0 J/pulse 1 Hz	15 min.	Film around microholes
20	Freon R-11 + H_2	1.0 torr 500 sccm each	3.0 J/pulse 1 Hz	15 min.	Film around microholes

X = 1% CF_4/ 1% F_2/ 98% He

All the Nd:YAG laser processed samples exhibited fringes surrounding microholes indicating thin film formation. However, an examination of these samples under SEM and wavelength dispersive x-ray microprobe showed no signs of fluorine or carbon. Raman spectroscopy also confirmed the absence of any form of carbon. We have also conducted experiments with and without gaseous precursor to identify the chemical reactions. It seems that no reaction occurred at the SiC

surface. High energy density of laser beam led to microhole drilling. Neither carbon nor fluorine was detected surrounding the microholes.

Rudder et al [21] claimed the growth of homoepitaxial diamond from the gaseous mixture 1% CF_4/1% F_2 in helium by thermally heating the substrate to 900°C. In our work with Nd:YAG, the SiC substrate was heated to various temperatures (due to the temperature gradient) but no evidence of diamond on SiC was observed.

4.2 Excimer Laser Photolytic Deposition

Since Nd:YAG laser pyrolysis did not induce deposition, we have considered photochemical decomposition of precursors using excimer lasers. Experiments were carried out first using a 23-nsec pulsed 248-nm KrF excimer laser and then with 17-nsec,pulsed 193-nm ArF excimer laser. Since the focused beam causes melting and microhole drilling, the beam was defocused to a point where the onset of melting of the surface layer occurred. The results of excimer laser study are described below.

SiC Substrate

Let us first examine the physics behind laser-gas-SiC interactions. The photon absorption of SiC substrate indicates that approximately 30% of laser energy will be absorbed at a wavelength 248 nm [23]. The binding energy of Si-C bond is 104 Kcal/mole and hence photodissociation of SiC into Si and C can readily occur both at 193 nm and 248 nm. The Si and C atoms released from photo and thermal dissociation can react with F and Cl radicals produced by the photodissociation of CCl_4 and F_2. F has a higher electronegativity than Cl and hence can react with Si and C to form SiF_4 and CF_4.

C-F	120 Kcal/mole
C-Cl	95 Kcal/mole
Si-F	129 Kcal/mole
Si-Cl	107 Kcal/mole

F atoms tend to chemisorb while Cl atoms can only physiorb. The interactions of laser photons cause electronic and vibrational excitation of F and thereby increase its sticking coefficient. The presence of atomic fluorine followed by the formation of appropriate CF_x radicals may allow the deposition of fluorinated diamond.

Initially Carborundum and Norton SiC were used as substrates. Figures 6a to c show three typical micrographs of laser irradiated zones. Wavelength dispersive X-ray analysis did not reveal the presence of carbon or fluorine in any of these zones. Raman spectroscopy also confirmed the absence of any form of carbon. Sample # 4 (Figure 6b), processed with low pulse rate (5 Hz), exhibited the same structural features as that of base SiC indicating no reaction. Increasing the pulse rate to 50 Hz (Sample # 5) appeared to have some effect but analysis of the laser irradiated zone revealed no positive results.

These data were surprising considering the fact that SiC is an excellent substrate for diamond growth and lasers were capable of decomposing the gases. Several experiments with varying process parameters were carried out. But the results remained same. Some possible explanations are:

1. The presence of impurities on the substrate surface may prevent the nucleation of carbon by surface catalytic reactions
2. The heterogeneous reaction rate of the gas decomposition at the SiC surface may be slow because of the chemical inertness of SiC.
3. The deposition time may not be adequate for the nucleation of carbon.

Since Carborundum and Norton SiC samples contained impurities, a high-purity grade SiC (EKasic HD, SiC = 99.5%) was procured from ESK engineered ceramics. This particular grade SiC, claimed by the manufacture, serves as the best substrate for diamond growth. Initial experiments using EKasic HD grade SiC as the substrate did not provide satisfactory results. Continued experimentation indicated that excimer laser growth of diamond film on SiC substrate is critically dependent upon laser parameters and purity of SiC. High energy densities of the order of 3 to 5 J/cm^2 are required to decompose the gases at SiC surface. In contrast, a pulse energy density of 0.7 J/cm^2 is sufficient to deposit carbon film on 440C stainless steel. Flowing gas at high rates followed by impingement of high energy density laser beam generated a film on SiC that consisted of a mixture of graphite and diamond (Figures 7 and 8). Excimer laser parameters included an energy density of 4 J/cm^2 and a pulse rate 100 Hz. The size of the film was 4 mm x 1.5 mm.

Numerous process conditions were then attempted with the objective of eliminating graphite phase from the deposited film. These variations include:

Wavelength		193 nm (ArF) and 248 nm (KrF)
Energy density		1 - 5 J/cm^2
Repetition rate		50 - 100 Hz
Gas flow	X	200-3000 sccm (gas)
	CCl_4	0.1-1 gm/min (liquid)
Total gas pressure		0.2 torr to atmospheric
Gas flow pattern		Simultaneous flow of both X and CCl_4, Injection of one gas after other
Gas preheating		20^{o}C to 1000^{o}C
Gas additive		O_2 at 50 sccm
Substrate preheating		20^{o}C - 500^{o}C
Deposition time		15 - 30 minutes

Over 25 experiments covering the effects of above-mentioned variables were carried out. The experimental conditions for representative samples are given in Table 7. Unlike that of hot-filament CVD grown diamond, laser CVD films exhibited ball-like morphological features of diamond and graphite structures rather than the typical octahedral features of diamond (Figure 9).

Wavelength Effect -- The rationale for using ArF wavelength (193 nm) was its ability to dissociate CCl_4 and F_2 more efficiently than KrF wavelength (248 nm). Results, however, indicated no major difference on the films grown using

Table 7. Excimer Laser CVD Experiments for SiC Substrate

Substrate: SiC Lens: 127 mm Focal Length

Sample No.	Laser Parameters	Precursor Gas	Preheating of Gas
57	193 nm, ArF 2 J/cm^2 50 Hz	X + H_2 + O_2	No
58	193 nm, ArF 2 J/cm^2 50 Hz	X + CCl_4	No
64	193 nm, ArF 2 J/cm^2 100 Hz	X + H_2 + O_2	No
65	193 nm, ArF 2 J/cm^2 100 Hz	X + CCl_4	No
73,74	248 nm, KrF 4 J/cm^2 100 Hz	X + H_2 + O_2	No
81,82	248 nm, KrF 4 J/cm^2 100 Hz	X + H_2 + O_2	Yes

X = 1% CF_4/1% F_2/98% He

either wavelength light. The films grown by 193-nm light had smaller coverage zones (due to the small spot size of ArF beam), possessed finer structures (Figure 10) and exhibited sharper peaks in Raman spectrum. Although 193-nm wavelength is a better choice, the drawbacks include the energy stability of the beam in the laser cavity, use of vacuum (or inert gas) in the beam delivery system, and smaller beam.

Energy density -- Energy density of the laser beam was found to play a significant role on the adhesion and coverage area of the film. In this work, energy density was varied by changing the beam size (through defocusing of the beam) rather than changing the pulse energy. Adhesion of the film was substantially improved (as determined in the friction test) by using higher energy density possibly due to increased substrate temperature. Better film quality in terms of Raman spectrum peaks was also obtained. But the coverage zone was small (as low as 3 mm x 1 mm).

Repetition rate -- Repetition rate has influenced the film thickness through its effects on chemical reactions. Laser pulses with repetition rates less than 50 Hz did not produce useful films. Higher repetition rate (> 50 Hz) increased the coverage zone and should be used wherever possible. This is quite different from laser ablation where low repetition rates (< 10 Hz) are often used.

Gas flow rate -- The volumetric or mass flow rate of the precursor gases is important for laser-gas reactions. Typically a gas flow of 1000 to 3000 sccm for X and about 0.1 to 1 gm/min for CCl_4 were found to be satisfactory. If the gas flow is not properly adjusted, there is no reaction at the substrate surface. It should be worth mentioning that a small plasma jet forms at the laser-gas interaction zone only at the flow rates specified. The effect of gas flow injection was also investigated. Experiments involving simultaneous flow of CCl_4 and X, delivery of X for 5 minutes followed by flow of CCl_4 (or vice versa) for 5 minutes were carried out. The resulting differences were negligible.

Gas pressure -- The gas pressure in the CVD chamber should be held less than 10 torr. Higher gas pressure generally leads to the complete absorption of laser beam energy before it reaches the substrate surface.

Substrate preheating -- Substrate preheating upto 550°C did not affect the film growth process.

Deposition time -- Deposition time was held less than 30 minutes because of the high repetition rate of the laser beam. An increase in the film thickness was noted with an increase in deposition time.

Gas Preheating -- It did not have any effect on the film formation (Figure 11) and on Raman spectrums.

Oxygen addition -- Addition of oxygen was beneficial in enhancing diamond structures.

Raman spectroscopy analysis of all the 25 samples revealed the presence of a mixture of diamond, DLC and graphite in laser irradiated regions. Figures 12 through 16 are representative Raman spectrums of laser grown films while Figure 17 is a spectrum of hot filament CVD deposited diamond film (on silicon substrate). Figure 17 is only for comparison purposes. The following conclusions may be drawn from Raman analysis.

Diamond and DLC films were deposited irrespective of the precursor gases being $X + H_2 + O_2$ or $X + CCl_4$ (Figures 12 and 13). However the films contained some SiC peaks. An increase in the pulse repetition rate from 50 Hz to 100 Hz (compare samples 57 with 64, and 58 with 65) eliminated SiC peaks from the Raman spectrums. Addition of oxygen to the precursor gases reduced the graphite growth (based on the ratio of diamond and graphite peaks in samples 57 and 64). Furthermore, $X + H_2 + O_2$ serves as a better precursor than $X + CCl_4$. A significant feature is that 193 nm-ArF beam is more efficient than 248 nm-KrF in depositing fluorinated carbon films (compare Figure 14 with Figure 16).

Wavelength dispersive X-ray analysis of samples clearly showed the presence of fluorine in addition to carbon, oxygen and silicon (Figure 18). However XPS analysis would be more useful in obtaining additional information and hence was conducted on two representative samples namely sample 64 (ArF-beam processed) and 74 (KrF-beam processed). For baseline comparison, SiC substrate was also examined. A large number of XPS spectrums were taken and analyzed. A summary of XPS data is given in Table 8. Figures 19 through 21 are the full scale spectrums of substrate, samples 64 and 74.

XPS data shows that laser grown films contained carbon and large amount of fluorinated carbons. An interesting observation is the absence of Si and its compounds near the edge of laser grown film thereby indicating a thicker film at the edge. XPS data in conjunction with Raman spectrums show that Sample 64, processed with ArF-beam, contained less graphite and graphite-fluoride compounds than Sample 74, processed with KrF-beam.

In summary, a mixture of diamond, graphite and C-F compounds could be deposited on SiC substrates. Variation of laser parameters and other experimental conditions did not completely eliminate the graphite. Graphite content could be minimized by the addition of oxygen and using ArF laser beam. Results further indicated that fluorine was not capable of etching the nondiamond phases possibly due to low volume percent of fluorine. It appears that removal of graphite requires atomic hydrogen or significanc quantities of fluorine. Additionally CF_3 and CCl_3 radicals may not have been present in sufficient quantities for the preferential growth and stabilization of diamond.

Table 8. XPS Analysis of Laser Grown Films

Sample/Location	Elements/compounds	Observations/comments
SiC substrate	Si, SiC, SiO_2, $Me_3SiSiMe_3$, $Me_3SiOSiMe_3$, $(Me_2SiO)_5$, Al_2O_3	SiO_2 is inherently present
Sample 74-Center of laser grown film	C, Si, SiO_2, various C-F and Si compounds	No SiC; Graphite and Graphite-fluoride
Sample 74-Edge of laser grown film	C and various C-F compounds	No Si or SiC; Graphite and Graphite-fluoride
Sample 64-Center of laser grown film	C, Si, SiO_2, various C-F compounds	No SiC; Si and SiO_2 have increased; SiF_6^{2-} exists; less graphite
Sample 64-Edge of laser grown film	C and various C-F compounds	No Si or SiC; more C and F; less graphite

440C Stainless Steel Substrate

Table 9 lists the experimental conditions used to deposit diamond films on steel substrates. Figure 22 is a typical SEM micrograph showing the dimensions of laser grown film on steel substrate.

Table 9. Excimer Laser CVD on Steel Substrates

Laser: KrF, 248 nm — Lens: 100 mm focal length
Substrate: 440C Stainless steel — Substrate Preheat: None

Sample No.	Precursor Gas Mix.	Pressure /Flow	Laser Parameters	Deposition Time	Comments
35	X	10 torr 3000 sccm	340 mJ, 50 Hz 50 mm defocus	15 min.	Green plume, Black film
36	X + H_2	10 torr 3000 sccm	335 mJ, 50 Hz 50 mm defocus	15 min.	Green plume, Black film
38	X + CCl_4	2 torr CCl_4 1 g/m X 3000 sccm	315 mJ, 50 Hz 50 mm defocus	15 min.	Film formation
40	CCl_4 + H_2	0.5 torr CCl_4 1 g/m	310 mJ, 50 Hz 50 mm defocus	15 min.	Black film
46	X + CCl_4 + H_2	2 torr X 3000 sccm CCl_4 1.5 g/m	220 mJ, 100 Hz 50 mm defocus	15 min.	Black film
50	Repeat 46 at 300 mJ for 30 minutes				Black film

Figures 23 and 24 show SEM micrographs of samples 35 and 50 illustrating the ball-like morphology of diamond and other carbon structures. Figures 25 through 29 are the Raman spectrums of steel samples showing peaks for diamond, diamond-like carbon and graphite. In addition, a strong, broad peak centered at 950 cm^{-1} is also observed. The effect of wavelength of laser beam is similar to that observed in SiC substrate. ArF beam laser CVD yielded much better Raman spectrums than KrF beam laser CVD (compare Figures 30a and b). It should be emphasized that the peak usually occurring at 950 cm^{-1} is absent in ArF-beam processed samples.

Visual, SEM, WDAX, and Raman spectroscopy analysis clearly showed that the films grown with numerous combinations of process variables did not eliminate the simultaneous growth of various forms of carbon. Etching of non-diamond phases by fluorine apparently is not efficient. It should be noted that we have used only 1% F_2 in gases and may not have been sufficient to remove the graphite.

The significant differences between SiC and steel substrates are: the film grown on SiC exhibited diamond and graphite peaks in Raman spectrum while the film on steel showed peaks for diamond, graphite, diamond-like carbon and an unidentified peak at 950 cm^{-1}. In addition, the peaks in Raman spectrum for films grown on SiC had higher intensity (counts) than for steel. Laser CVD experiments have also demonstrated that SiC, obtained from ESK engineered ceramics, is a better substrate than 440C steel for diamond growth.

4.3 Solid Lubrication Behavior

According to solid lubrication theory [24], the friction coefficient (f) of solid lubricants can be related to the film shear strength (S), applied load (P) and elastic modulus (E) by means of the following expression:

$$f = K\ S\ P^{-0.33}\ E^{-0.67}$$

where K is a constant. Diamond films are excellent for carrying high contact loads but suffer from problems of providing low shear film and tendency to oxidize and to graphitize at temperatures above 800°C. Diamond fluorination can alleviate such problems by providing low shear strength film through the formation of C-F compounds and by passivating the surface from adsorption of water or oxygen and thereby reducing friction. Fluorinated diamonds are excellent for atomic oxygen environment and other harsh operating environments. For example, blower motor bearings in chemical laser satellite communication systems are subjected to halogen atmosphere and can have improved performance through fluorinated diamond coating.

Laser CVD experiments provided a layer, of the order of 1 micron thickness, consisting of diamond, diamond-like carbon and graphite. Such thin films may be appropriate for solid lubrication purposes. The solid lubrication behavior of laser grown films on SiC and 440C steel was studied using the pin (or ball)-on-disc test rig. The pin was made of SiC with a diameter 6.4 mm while the disc was a hardened tool steel. Results and tribosystem conditions are given in Table 10 for SiC. A major problem experienced during friction testing is establishing the full face contact between SiC pin and the disc mostly due to the nonuniformity of the pin geometry. In all the experiments, the face contact was less than 20%. Table 10 clearly indicates that, for a given set of tribotest conditions, uncoated SiC exhibits a friction of 0.534 and that laser coating substantially reduced the friction value. Experiments were repeated three times to determine the variations. Both the life of coating and the friction can be better if full face contact existed during tribotests.

For 440C steel, a ball-on-disc apparatus was used to evaluate the frictional characteristics of the film. 12 mm diameter bearing balls have been procured and deposited with fluorinated carbon films using ArF and KrF excimer lasers. The ball was laser coated 440C stainless while the disc was a hardened tool steel. Friction measurements were conducted as functions of load and sliding speed. Experiments were repeated three times and average values are tabulated in Table 11.

Table 10. Friction Data of Laser Grown Fluorinated Diamond/Graphite Films on SiC

Load = 4.6 N, Sliding speed = 80 mm/sec, Temperature = 20°C
Pin = SiC Disc = Hardened tool steel, R_a = 0.065 micron

Sample	Initial friction	*Mean friction	**Life of the coating in meters
Uncoated	0.534	0.534	---
Laser Coated	0.118	0.310	17.0
	0.139	0.321	16.7
	0.203	0.256	20.9

** Life of the coating is defined as the sliding distance before the coefficient of friction exceeds 0.534
* Mean friction is defined as the friction at half life of coating

Table 11. Friction Data of Laser Grown Fluorinated Diamond/Graphite Films on 440C Stainless Steel

Sample	Load, N	Speed, mm/s	Initial friction	Mean friction	*Life, meters
Uncoated	2.36	132	0.3	0.8	0.1
	2.36	66	0.25	0.5	0.8
	4.60	66	0.25	0.5	0.4
ArF-laser Coated	2.36	132	0.12	0.25	3.0
	2.36	66	0.15	0.21	2.3
	4.60	66	0.21	0.30	1.6
KrF-laser coated	2.36	66	0.17	0.24	7.0
	4.60	66	0.19	0.26	4.0

* Life is defined as the sliding distance before the friction exceeds 0.5

The variation of coefficient of friction as a function of sliding distance for uncoated balls shows that the friction value rapidly increased with the sliding distance. After sliding for a distance of less than 0.1 m, the friction was increased to about 0.8 which is unacceptable for practical applications. Uncoated balls are tested for baseline comparison. Laser deposited films exhibited much lower friction under identical conditions. Data indicate that the fluorinated carbon films have a friction coefficient in the range 0.12 -0.18 for a long sliding distance. KrF-beam processed films had longer life than ArF-beam processed films but the friction values were relatively higher.

It is appropriate to say that our friction experiments involved high contact stress and high speed conditions. By comparison, the friction data of soft metal and PTFE films, reproduced in Figure 31 from Reference 6, were obtained

using a pin-on-disc (low stress conditions compared to our ball-on-disc test) at speeds of the order of 1-3 mm/sec (in contrast to 66-132 mm/sec as in our tests). Sliding speeds of 1-3 mm/sec represent more closely those speeds occurring in the microslip areas of ball bearings in space applications [6].

Our data in comparison with Figure 31 shows that fluorinated carbon films deposited via laser technique are as effective solid lubricants as soft lead and PTFE, and can be used at severe rubbing conditions. It is worth mentioning that fluorinated carbon can be used at high temperatures over lead and PTFE films. A comparison of our friction data can also be made with the data given by Miyake et al [7] who deposited films consisting of a mixture of diamond and graphite on various substrates using a plasma CVD technique and by Kustas et al [8] who deposited amorphous carbon/graphite coating on 440C steel via ion beam technique. Both investigators used a reciprocating motion friction tester at low speeds. Results of their studies on 440C stainless steel substrate, reproduced in Figure 32, indicate a friction coefficient of about 0.15 to 0.25.

Friction and wear data of single crystal diamonds, sintered diamond composites and diamond-like carbon films have been well documented in many publications. All these studies indicated that diamond-like carbon exhibits lower friction than diamond mostly due to the presence of entrapped hydrogen. The surface chemistry of the films plays a major role in determining the tribological properties. Diamond surfaces with adsorbed oxygen and moisture yielded high friction (0.5 to 0.8) and those saturated with hydrogen yielded low friction 0.1 [5]. Intrinsic alteration of the diamond surface such as hydrogenation and fluorination is needed to provide passive surfaces. Recently Miyake and Kaneko [9] demonstrated that fluorinated Si/C films were effective in tribology by reducing surface energy through the increased contact angle of water, by reducing the microwear on atomic scale and eliminating friction force fluctuations.

In summary, friction test results are highly promising in Phase I work and laser grown fluorinated carbon films can be a potential solid lubricant.

5. ESTIMATES OF PHASE I TECHNICAL FEASIBILITY FOR PHASE II

Phase I research was designed to synthesize fluorinated diamond films and determine their tribological behavior. The project work resulted in the successful development of a simpler and faster process for growing a mixture of fluorinated diamond and graphite films. Efforts in eliminating the nondiamond phases were not completely successful. However, the application of this project is aimed at solid lubrication, a mixture of diamond, graphite and diamond-like carbon films may be better suited than pure diamond. Limited tribological tests in Phase I proved the effectiveness of laser grown fluorinated carbon films as solid lubricants.

The project is technically feasible from the perspective of solid lubrication and lends itself as an economically competing method for depositing uniform, continuous, high quality diamond-like films on nondiamond substrates. Laser CVD process can be easily automated. Laser technology for diamond coatings is in "infant" stages and requires active research for commercial success.

Phase I research provided the basic data needed on the growth and tribology of fluorinated carbon films. Based upon the guidelines from Phase I work, Phase II will investigate the following:

1. **Scaling up the process**

    a. Optimization of precursor, gas flow, laser parameters, substrate temperature, window cleaning etc
    b. Deposition on contoured surfaces using stationary focused beam/moving substrate

2. **Studies of solid lubrication**

    a. Changes in surface chemistry, effects of temperature and reaction gases on the tribosurface chemistry
    b. Film formation and wear
    c. Shear strength
    d. Substrate effects
    e. Film thickness
    f. Film rheology (viscous flow, plastic flow, interface at the substrate/film)
    g. Adhesion

3. **Bearing tests and evaluation**

    a. Relationships among cage wear, ball or race wear
    b. Transfer film buildup as functions of load, speed, temperature and atmosphere
    c. Torque behavior as a function of revolutions
    d. Performance and degradation behavior of fluorinated carbon films in vacuum, atomic oxygen, UV, thermal cycling and laser threat environment

6. POTENTIAL TO DoD

Current and future military space system components performance, life and reliability can be substantially improved by the development of new tribomaterials. The moving mechanical assemblies in ground combat systems (diesel cylinder, turbocharger, transmission/steering, and turbine regenerator) aircraft and missiles (bearing-rotor systems, IR detection systems and turbines) and space systems (satellite pointing-control systems, surveillance sensor cooling system, space propulsion) will significantly benefit from the Phase I research. Solid lubricated ceramic bearings may be the ultimate solution for many tribosystem problems in space applications. Phase I research namely laser CVD technique of depositing fluorinated diamond will provide payoffs for such applications

Space based mission requirements in acquisition, tracking and pointing, IR surveillence, laser radar and communication and chemical propulsion indicate many tribological problems including: high-temperature synthetic lubricants; material for solid-lubricated, rolling element bearings; damage-tolerant, corrosion-resistant surface modification methods; tribochemistry in ball/cage, cage/land and ball/race interactions; and lubricant distribution. Some of these tribological needs can be successfully met by this project.

Fluorinated carbon films developed in Phase I effort should compete with the effective space lubricants including MoS_2, lead and PTFE. MoS_2 and PTFE are generally restricted to low contact stresses, low humidity and light duty applications where torque noise must be minimal. Lead can be used from low to heavy contact stress where torque noise is not so critical. All three lubricants can not be used for high-temperature applications. Fluorinated carbon films appear to serve better than these three lubricants in meeting the stringent demands of space bearings.

A comprehensive handbook on space lubrication was provided by NASA in 1985 [25]. Information on the data associated with different types of lubricants are available in this handbook. A study of this book indicates the need for newer lubricants that can withstand extremely different service conditions coupled with extended and sometimes demanding performance in strategic defense systems. Phase I results have potential to provide solution to space lubrication problems including ceramic roller bearings and high-temperature load dampers.

7. CONCLUSION

Phase I research led to the development of a laser CVD process for depositing a mixture of diamond, graphite and diamond-like carbon films on bearing material substrates including SiC and 440C stainless steel. A gaseous precursor mixture of halogenated methane and halogen, a Nd:YAG laser for creating photothermal effects and an excimer laser for generating photochemical reactions were employed for this purpose. The type of laser, carbon feedstock, laser-precursor gas interactions, and deposition conditions have been established. Scanning electron microscopy, wavelength dispersive X-ray analysis, and Raman spectroscopy analysis of laser grown films revealed that the films deposited on SiC consisted of a mixture of diamond and graphite and the films on 440C steel were composed of diamond, diamond-like carbon and graphite. Efforts to eliminate the graphite from the film were not successful. X-ray photoelectron spectroscopy (XPS) data showed the presence of significant amount of C-F compounds both in the surface and subsurface layers. Tribological tests (ball-on-disc and pin-on-disc) of laser grown films indicated a friction coefficient in the range 0.1 to 0.3 depending on the wear couple, sliding speed and load confirming the effectiveness of these films as solid lubricants for moving mechanical assemblies in space structures. Fluorination of carbon films has the following attributes: passivation of the surface of diamond/graphite films from adsorption of water or oxygen, reduction of surface energy needed for shearing of the film during solid lubrication, and protection from corrosive environments. A comparison of solid lubrication performance of laser grown fluorinated carbon films with MoS_2, PTFE and soft lead demonstrate the potential of fluorinated carbon for high-temperature and harsh chemical environments.

8. REFERENCES

1. L.L. Fehrenbacher, "Tribology Research and Development Needs of Advanced Military Systems," Engineered Materials for Advanced Friction and Wear Applications, Proc. of Int. Conf, Maryland, March 1988, ASM, 169
2. M.E. Campbell, J.B. Loser, and E. Sneegas,"Solid Lubricants," NASA-SP 5059, May 1966
3. M.B. Peterson and M. Kanakia,"Solid Lubricants", Engineered Materials for Advanced Friction and Wear Applications, Proc. Int. Conf, ASM, 1988, 153
4. T. Spalvins,"Tribological Advances in Aerospace Applications," ibid, 203
5. M.N. Gardos and K.S. Ravi,"Tribological Behavior of CVD Diamond Thin Films," in Proc. of Ist Int.Conf.on Diamond and Diamond-Like Films, (ed) J.P. Dismukes et al, 1989, 475
6. E. W. Roberts, "Thin Solid Lubricant Films in Space," Tribology International, Vol.23, No.2, 1990, 95
7. S. Miyake, S. Takahashi, I. Watanbe and H. Yoshihara,"Frictional and Wear Properties of Hard Carbon Composed of Diamond and Graphite Mixed Crystal Structure Deposited onto Various Substrates," Proceedings of the JSLE International Tribology Conference, July 8-10, Tokyo, Japan, 1985, 407
8. F.M. Kustas et al,"Tribological Performance of Hard Carbon Coatings on 440C Bearing Steel", Diamond Optics III, A. Feldman and S. Holly (eds.), SPIE, Vol. 1325, 1990, 116
9. S. Miyake and R. Kaneko, "Micro-tribological Properties and Applications of Superhard and Lubricating Coatings", Applications of Diamond Films and Related Materials, Y. Tzeng, M. Yoshikawa, M. Murakawa and A. Feldman (eds.), Elsevier Science Publishers, 1991, 691
10. Applications of Diamond Films and Related Materials, Y. Tzeng, M. Yoshikawa, M. Murakawa and A. Feldman (eds.), Elsevier Science Publishers, 1991
11. Y. Goto , T. Yagi, and H. Nagai, "Synthesis of Diamond Films By Laser-Induced Chemical Vapor Deposition," Materials Research Society Proceedings, V.129, 1989, 213
12. G. Y. Tyndall and N.P. Hacker,"KrF Laser-Induced CVD of Diamond," Presented at 1990 Materials Research Society, November 1990
13. F.G. Celii, H.H. Nelson, and P.E. Pehreson,"The Effects of UV Laser Irradiation on the Filament-assisted Deposition of Diamond", Journal of Materials Research, 5, 1990, 2337
14. B.C. Janvrin,"Laser Chemical Vapor Deposition of Diamond Films", M.S. thesis, Iowa State University, 1990
15. P. Molian and A. Molian,"CO_2 Laser Deposition of Diamond Thin Films", To appear in Jouranl of Materials Science, 1992
16. S.L. Thaler,"Laser Detonation DLC Films", Applications of Diamond Films and Related Materials, Y. Tzeng, M. Yoshikawa, M. Murakawa and A. Feldman (eds.), Elsevier Science Publishers, 1991, 857
17. N.I. Chapliev et al,"Laser-Assisted Selective Area Deposition of Diamond Thin Films", Applications of Diamond Films and Related Materials, Y. Tzeng, M. Yoshikawa, M. Murakawa and A. Feldman (eds.), Elsevier Science Publishers, 1991, 417
18. J. Narayan, V.P. Godbole and C.W. White,"Laser Method for Synthesis and Processing of Continuous Diamond Films on Nondiamond Substrates", Science, 252, April 1991, 416

19. D.L. Patterson, R.E. Hauge, and J.L. Margrave, "Fluorinated Diamond Films, Slabs and Grits," Material Research Society Symposium Proceedings, 140, 1989
20. D. Bauerle, Chemical Processing With Lasers, (Springer-Verlag, Newyork, 1986)
21. R.A. Rudder, J.D. Post Hill, and R.J. Markunas,"Thermal CVD of Homoepitaxial Diamond Using CF_4 and F_2", Electronics Letters, August 1989, Vol.25, No.18, 1220
22. H. Okabe, Photochemistry of Small Molecules. John Wiley and Sons, 1978
23. M. Murahara, H. Arai and T. Matsumura,"Excimer Laser-Induced Etching of SiC", MRS Proceedings, V. 129, 1989, Laser and Particle Beam Chemical Processes on Surfaces (eds.) A. Johnson, G. Loper and T. Sigmon, 315
24. M.D. Kanakia and M.B. Peterson,"Literature Review of Solid Lubrication Mechanisms", Interim Report BFLRF No. 213 to U.S. Army Belvior Research and Development and Engineering Center, Fort Belvoir, VA, July 1987, 19
25. Lubrication Handbook for the Space Industry - NASA TM 86556, Dec. 1985

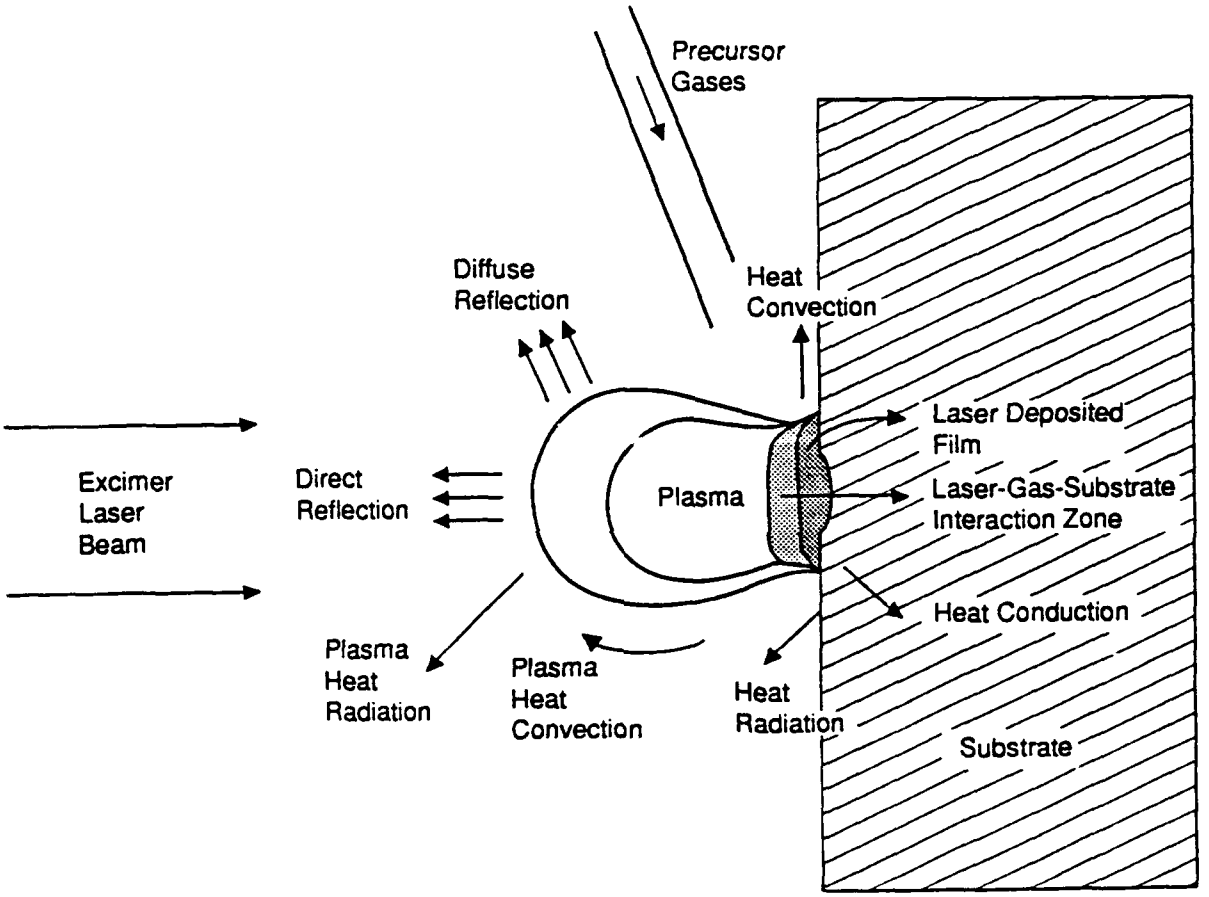

Figure 1. Laser CVD interaction processes during perpendicular irradiation of laser beam on the substrate surface

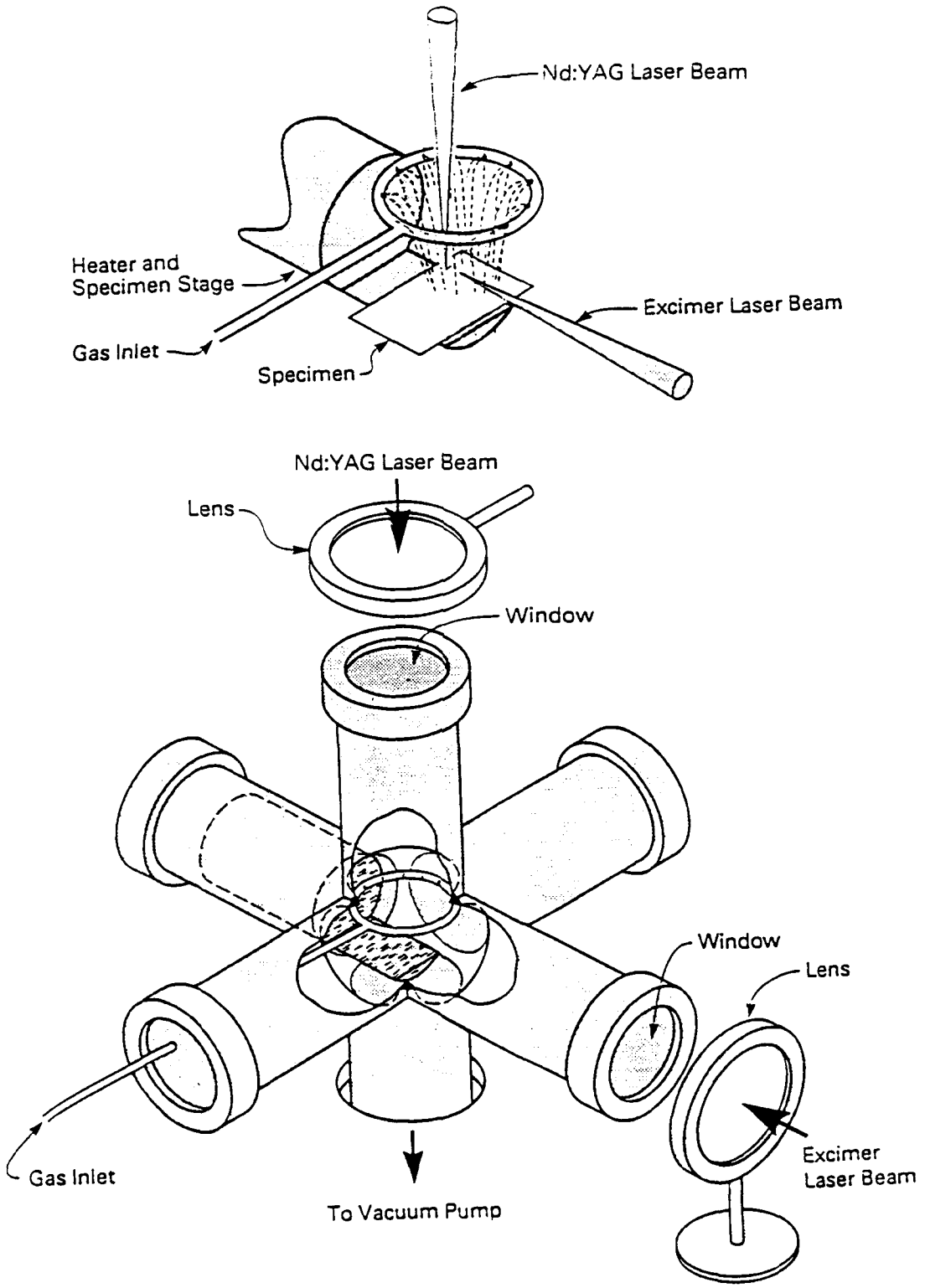

Figure 2. Schematic diagram showing laser CVD experimental set-up. A single laser beam (YAG or Excimer) was only used for each experiment

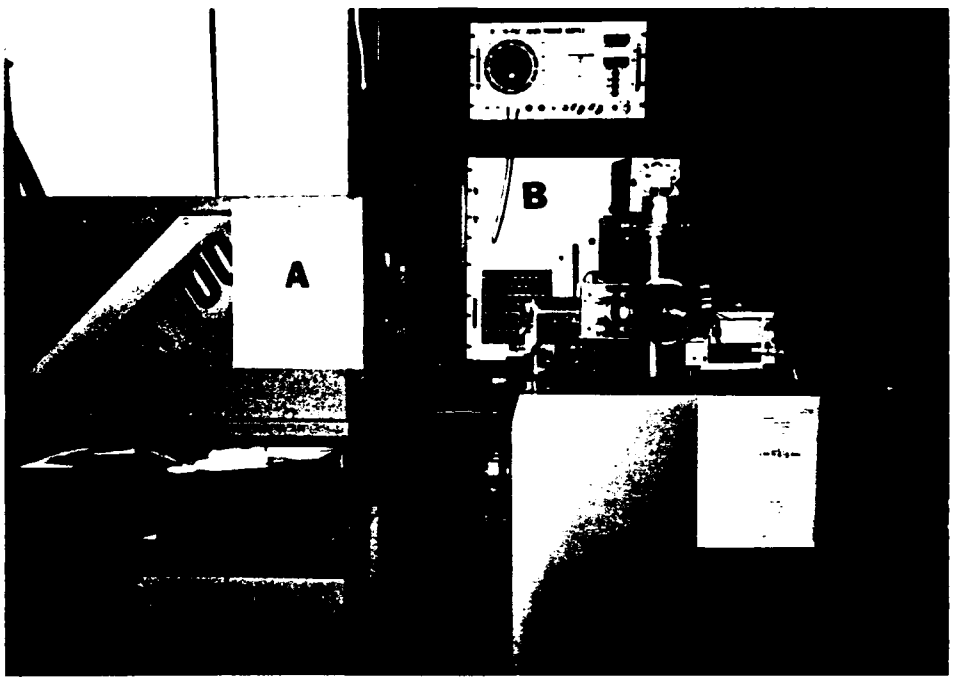

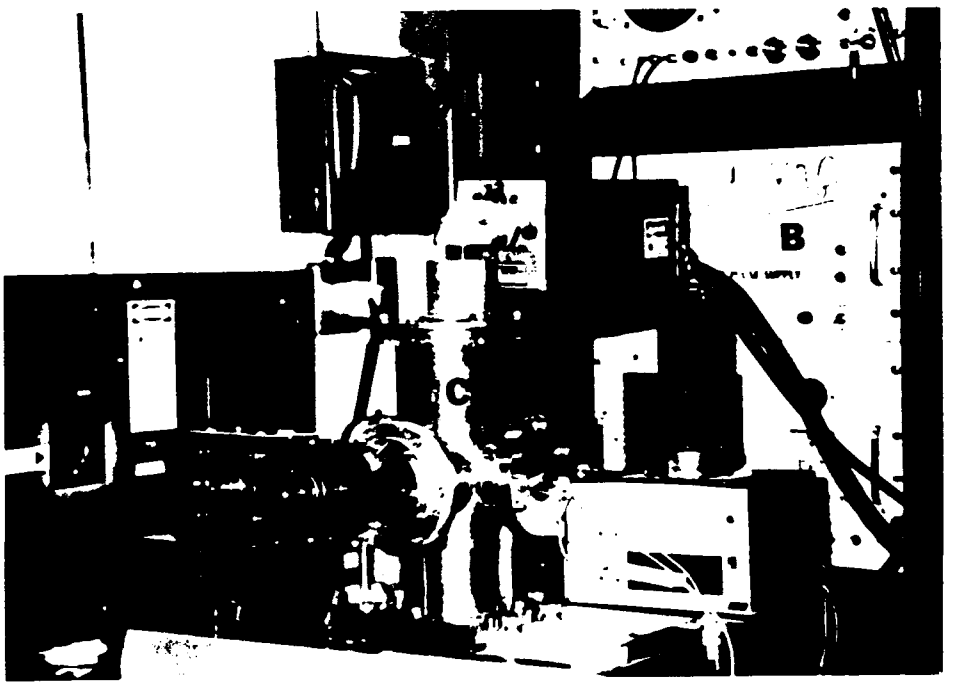

Figure 3. Photographs of laser CVD experiment. A: Excimer laser B: Nd:YAG laser, C: Vacuum chamber

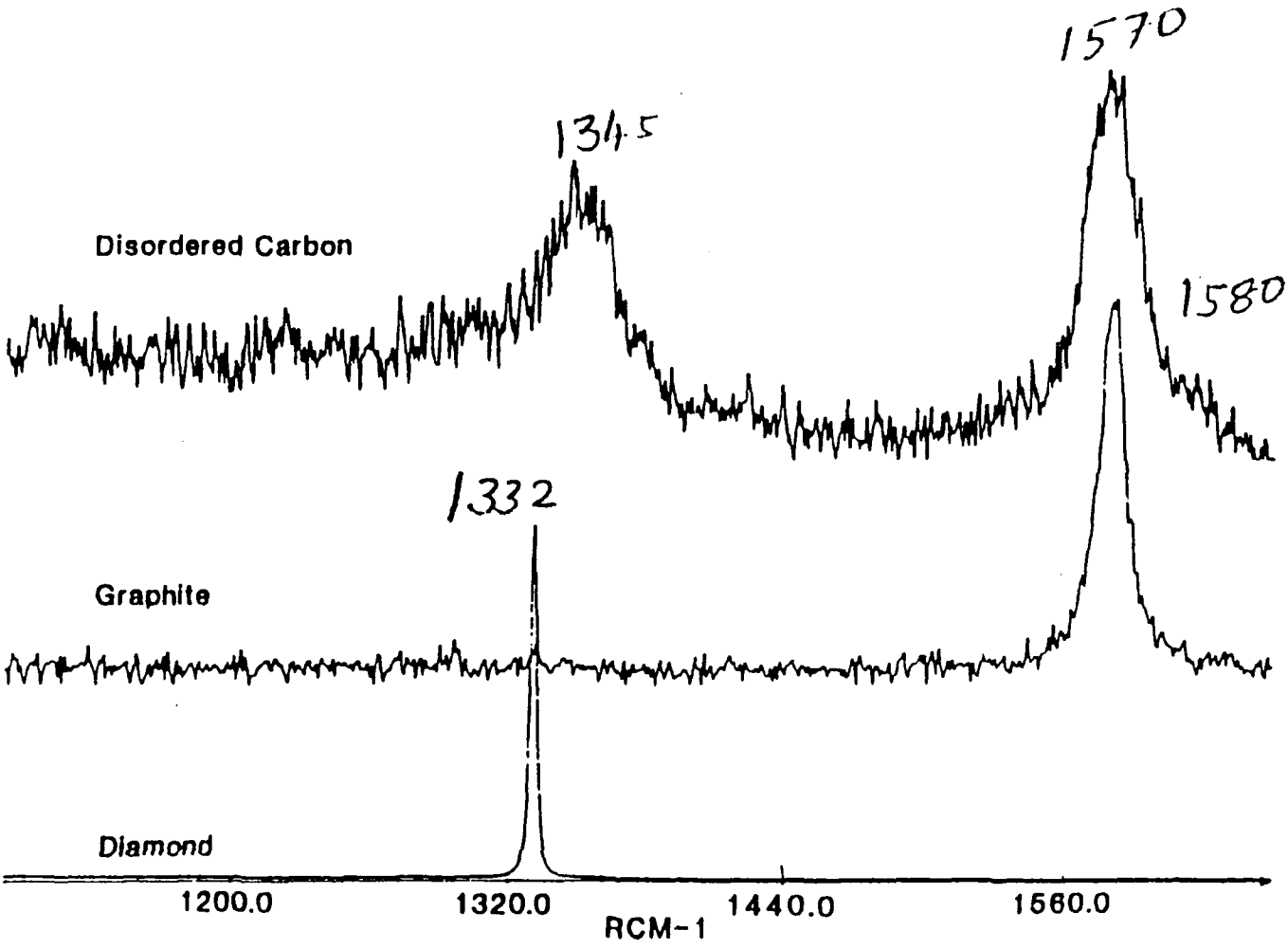

Figure 4. Reference Raman spectra for diamond, graphite and diamond-like carbon

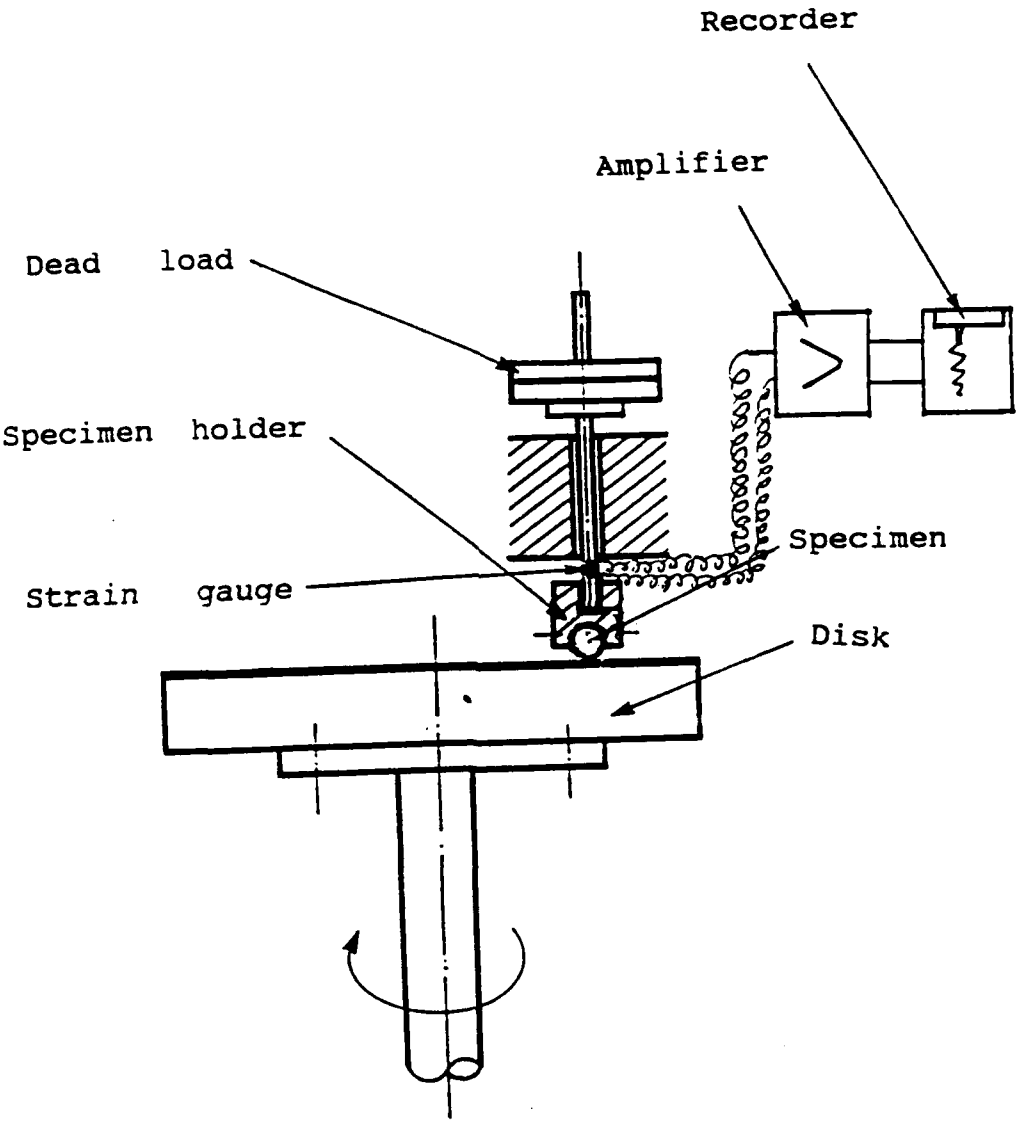

Figure 5. Schematic of ball-on-disc tribotest rig

a

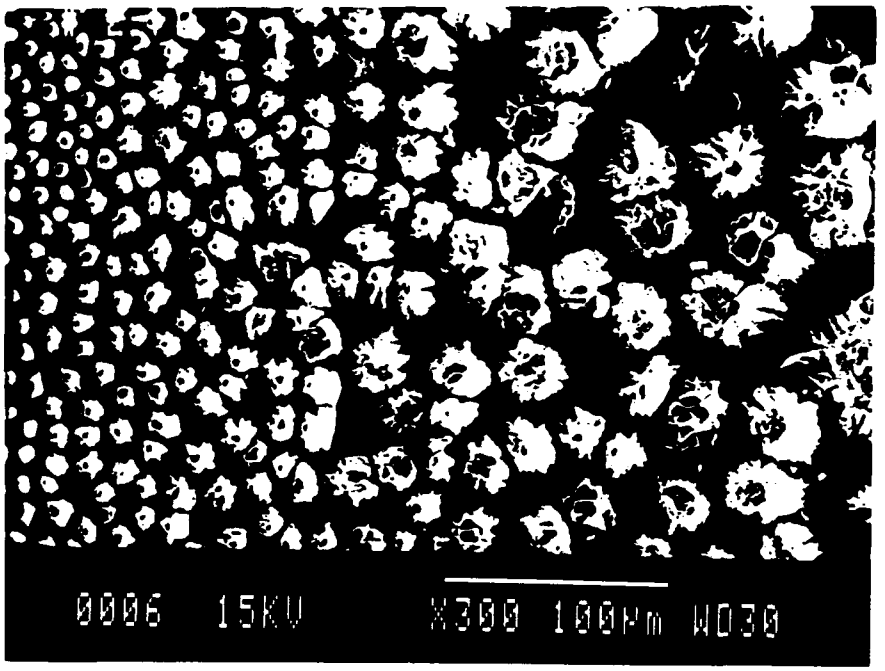

b

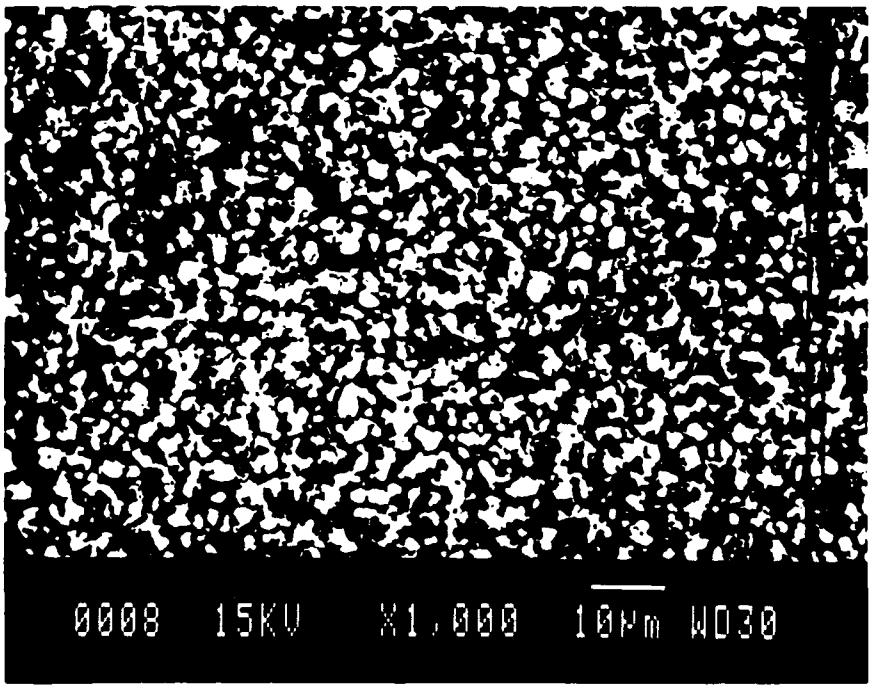

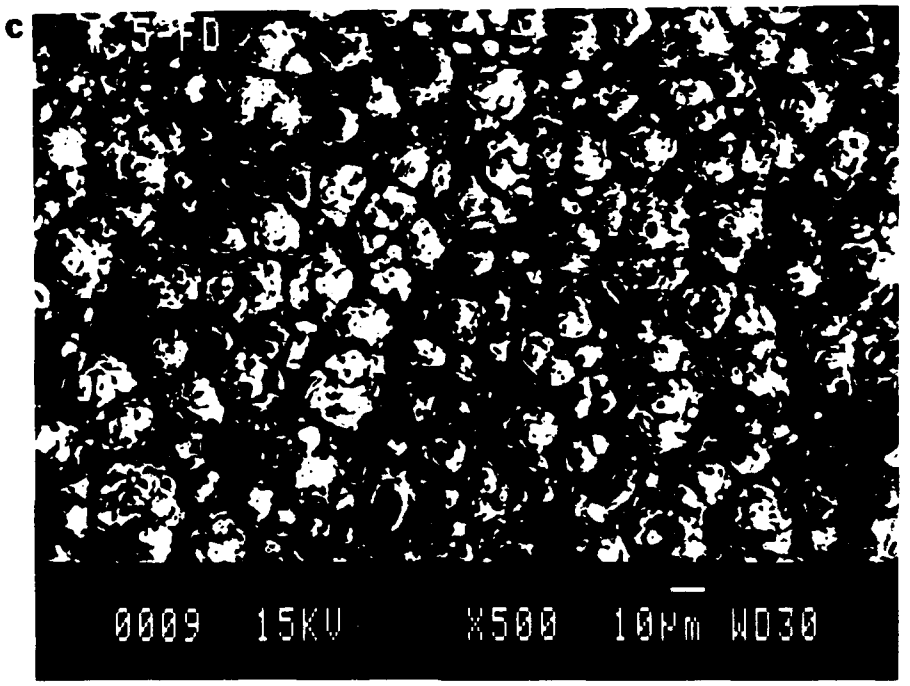

Figure 6. SEM micrographs of 248-nm KrF laser processed SiC (Carborundum) showing three different zones depending on the energy density and pulse rate (Precursor : X, Focal length of lens: 100 mm). No diamond or other forms of carbon and fluorine was identified in these zones.

(a) Sample # 2, 350 mJ, 5 Hz, 25 mm defocus
(b) Sample # 4, 310 mJ, 5 Hz, 40 mm defocus
(c) Sample # 5, 250 mJ, 50 Hz, 40 mm defocus

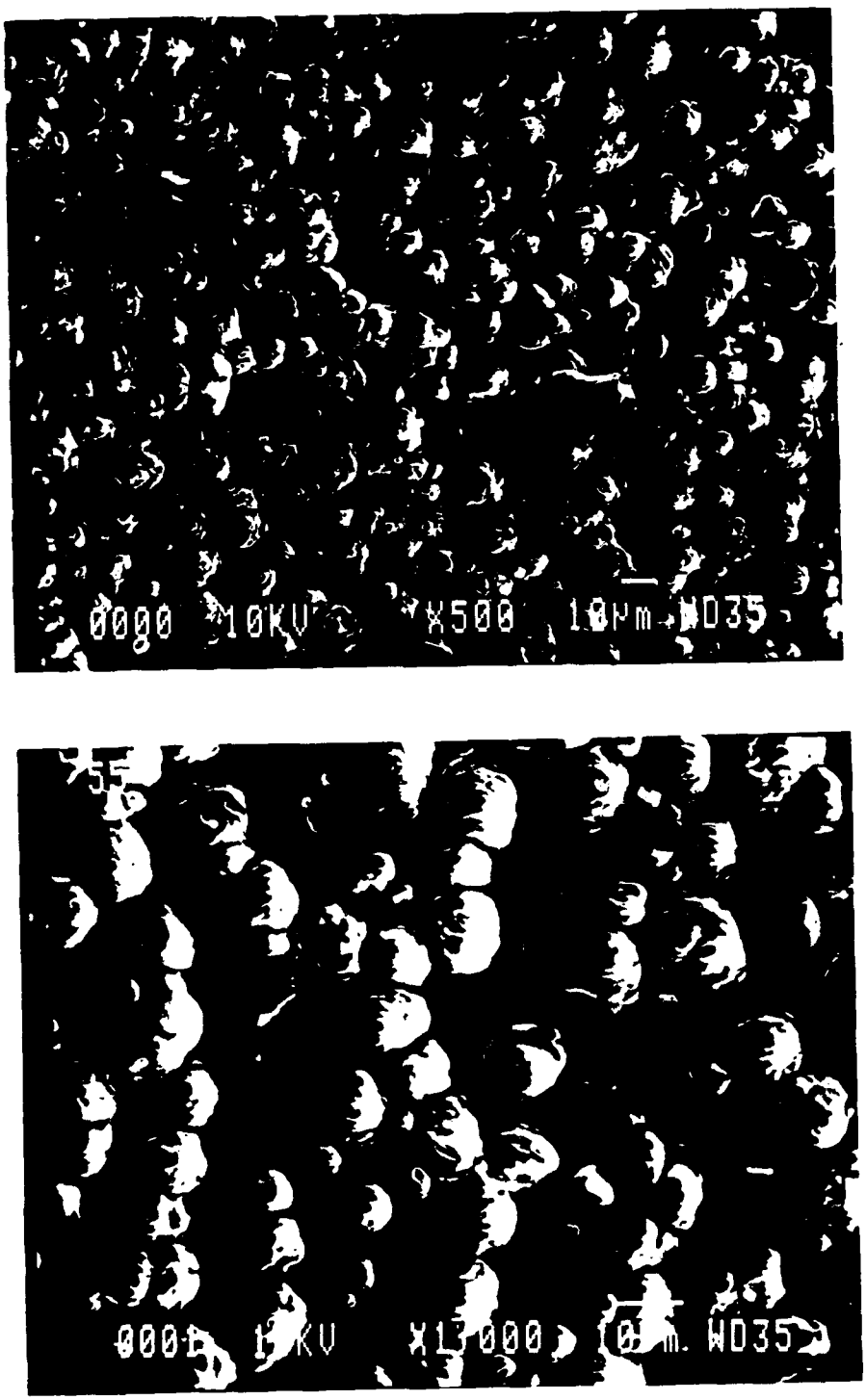

Figure 7. Scanning electron micrographs of Sample # 55 showing a mixture of fluorinated diamond and graphite on SiC substrate

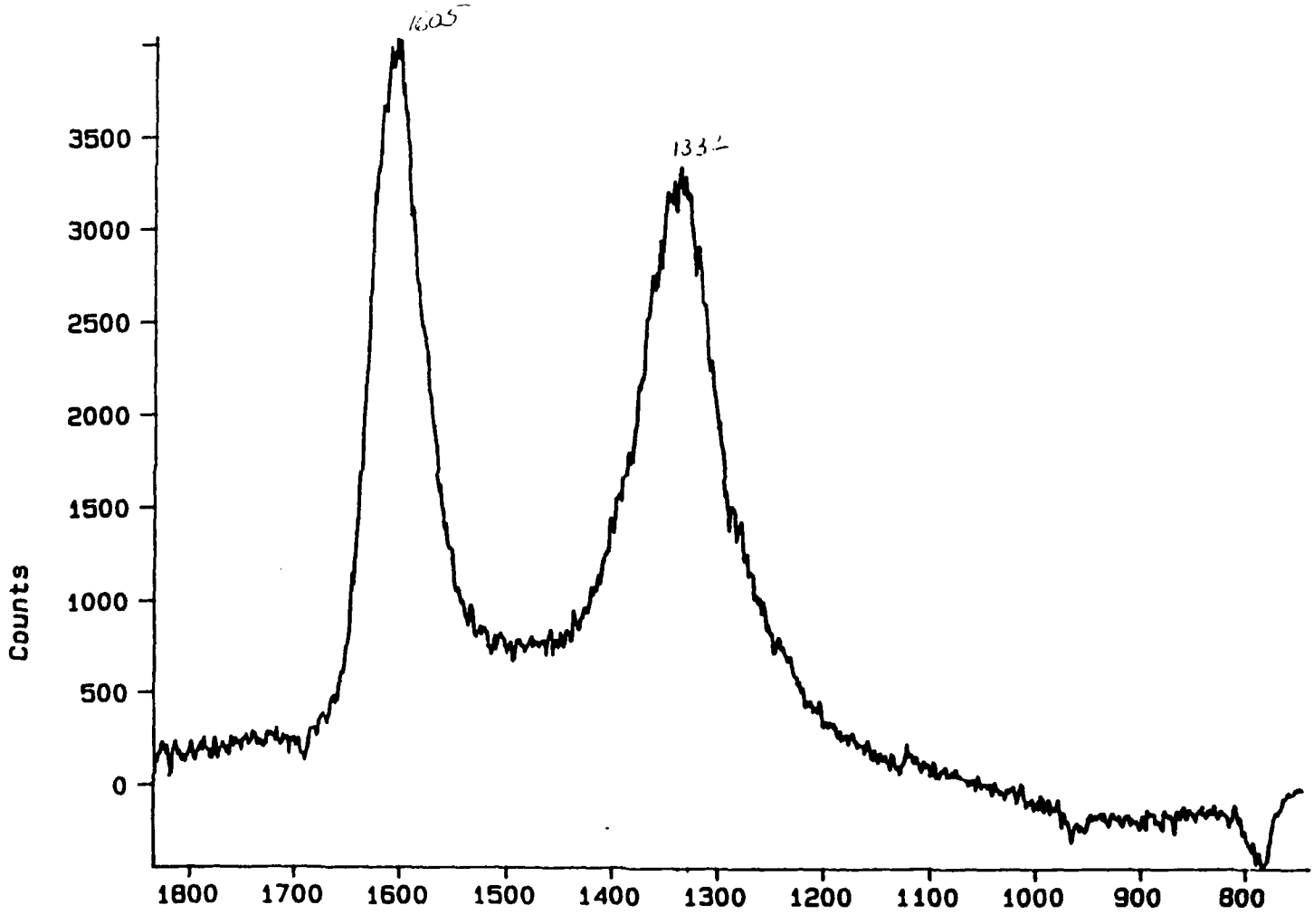

Figure 8. Raman spectrum of Sample # 55 showing the peaks for diamond and graphite. Note the absence of SiC peaks at 786 cm^{-1} and 965 cm^{-1}.

a

b

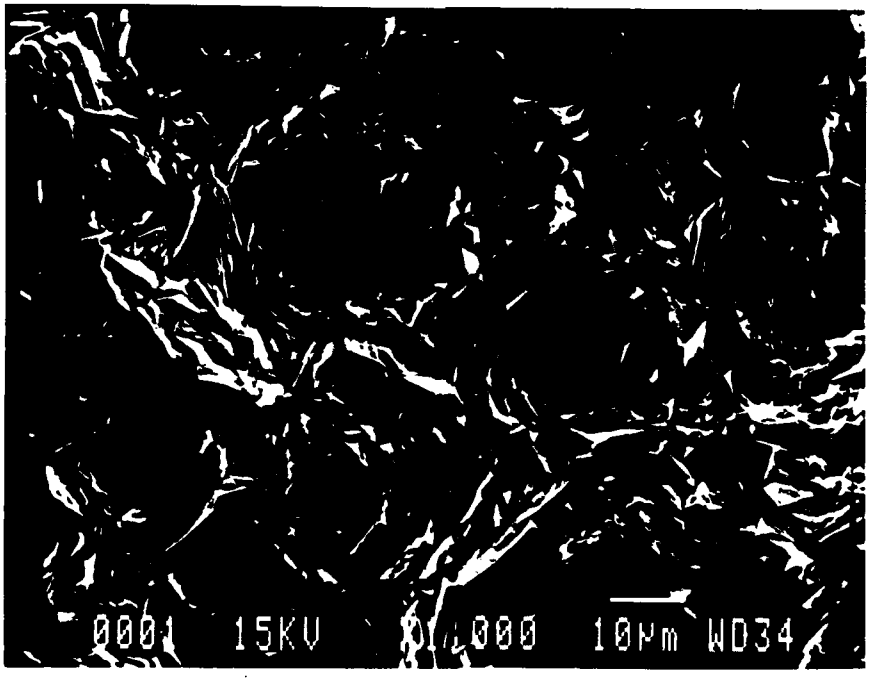

Figure 9. Scanning electron micrographs of diamond films
(a) Laser grown film on SiC
(b) Hot filament CVD grown film on Si

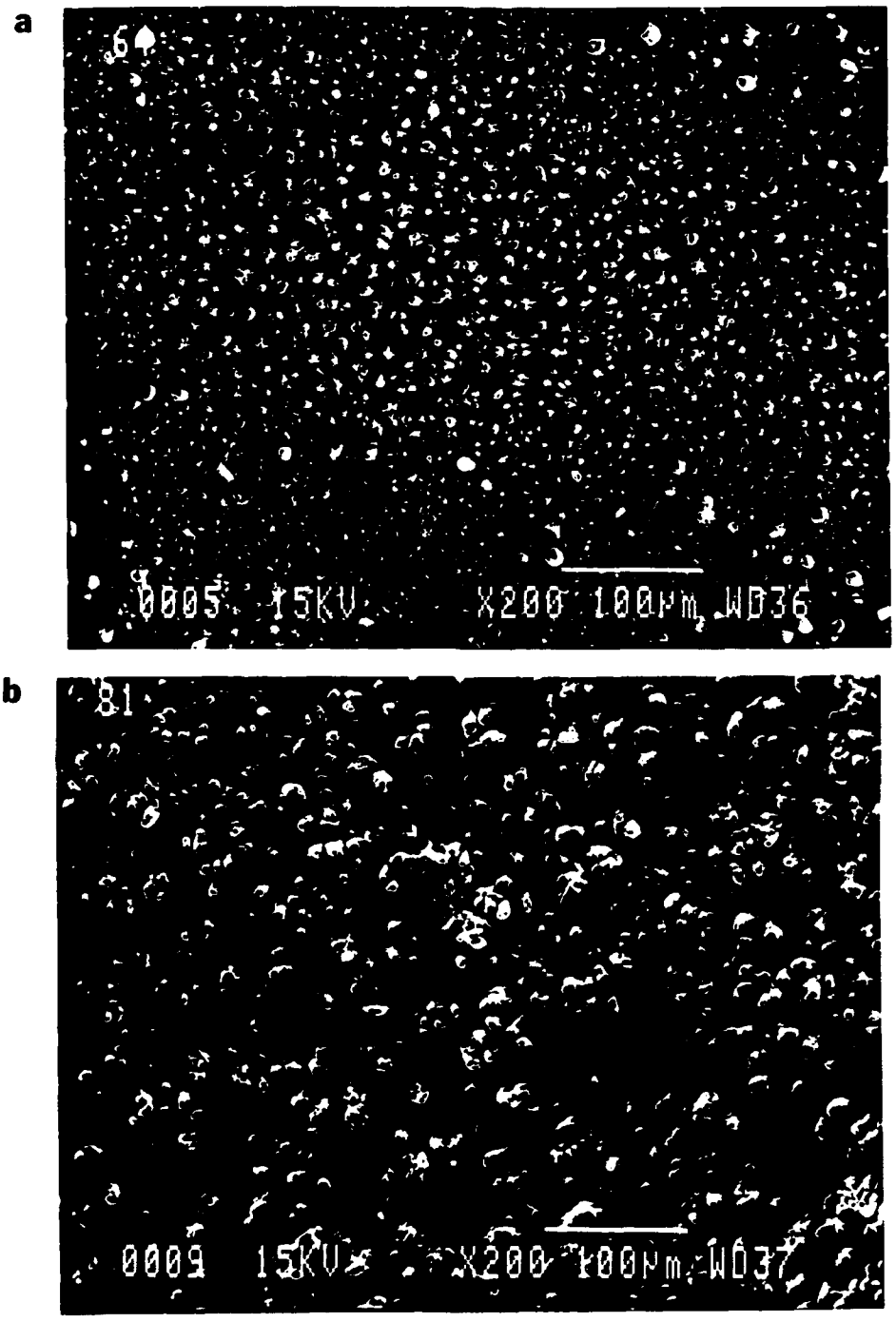

Figure 10. Scanning electron micrographs of laser grown films on SiC substrate
(a) 193-nm ArF beam processed
(b) 248-nm KrF beam processed

a

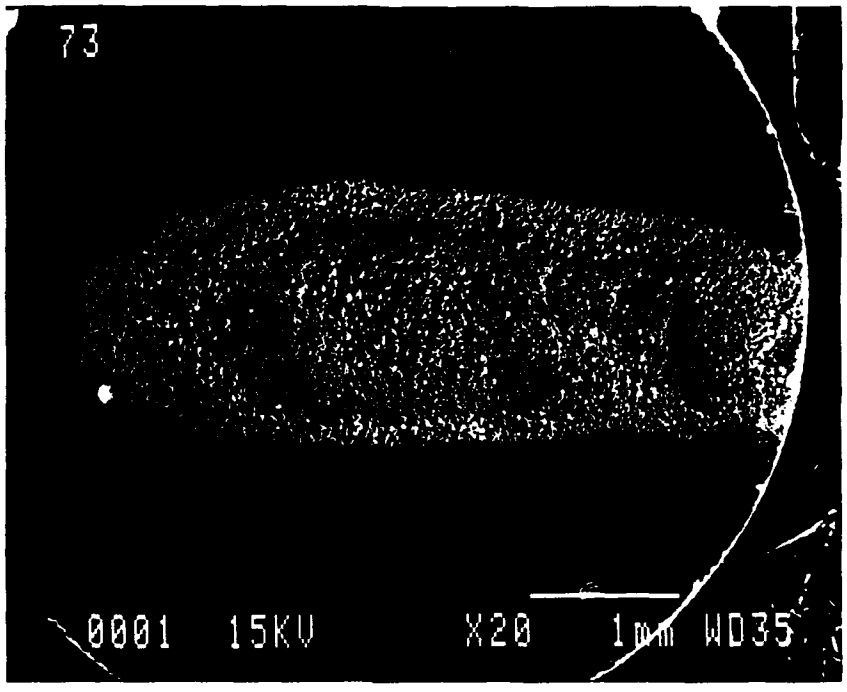

b

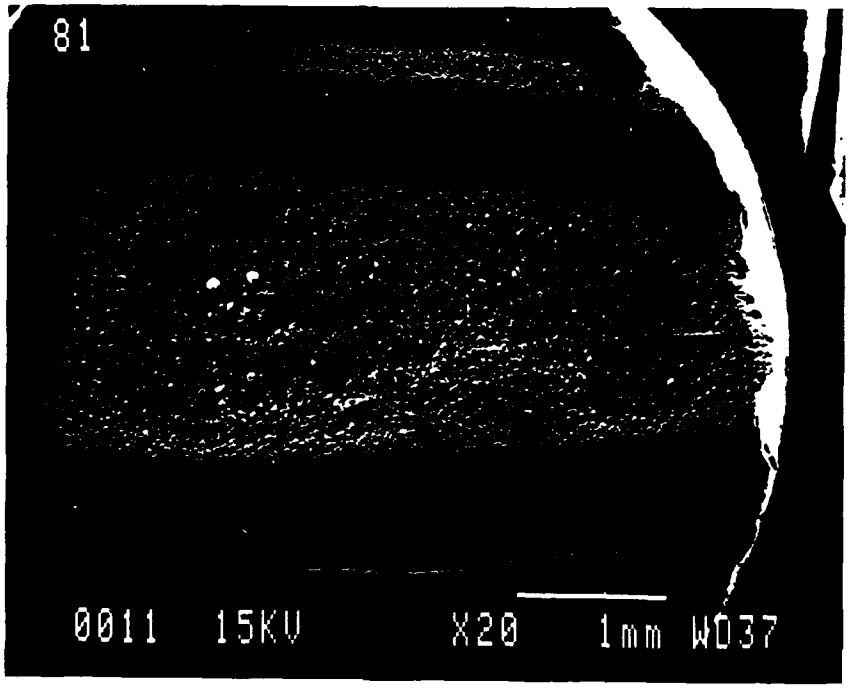

Figure 11. Scanning electron micrographs of laser grown films on SiC
(a) Without gas preheating
(b) With gas preheating

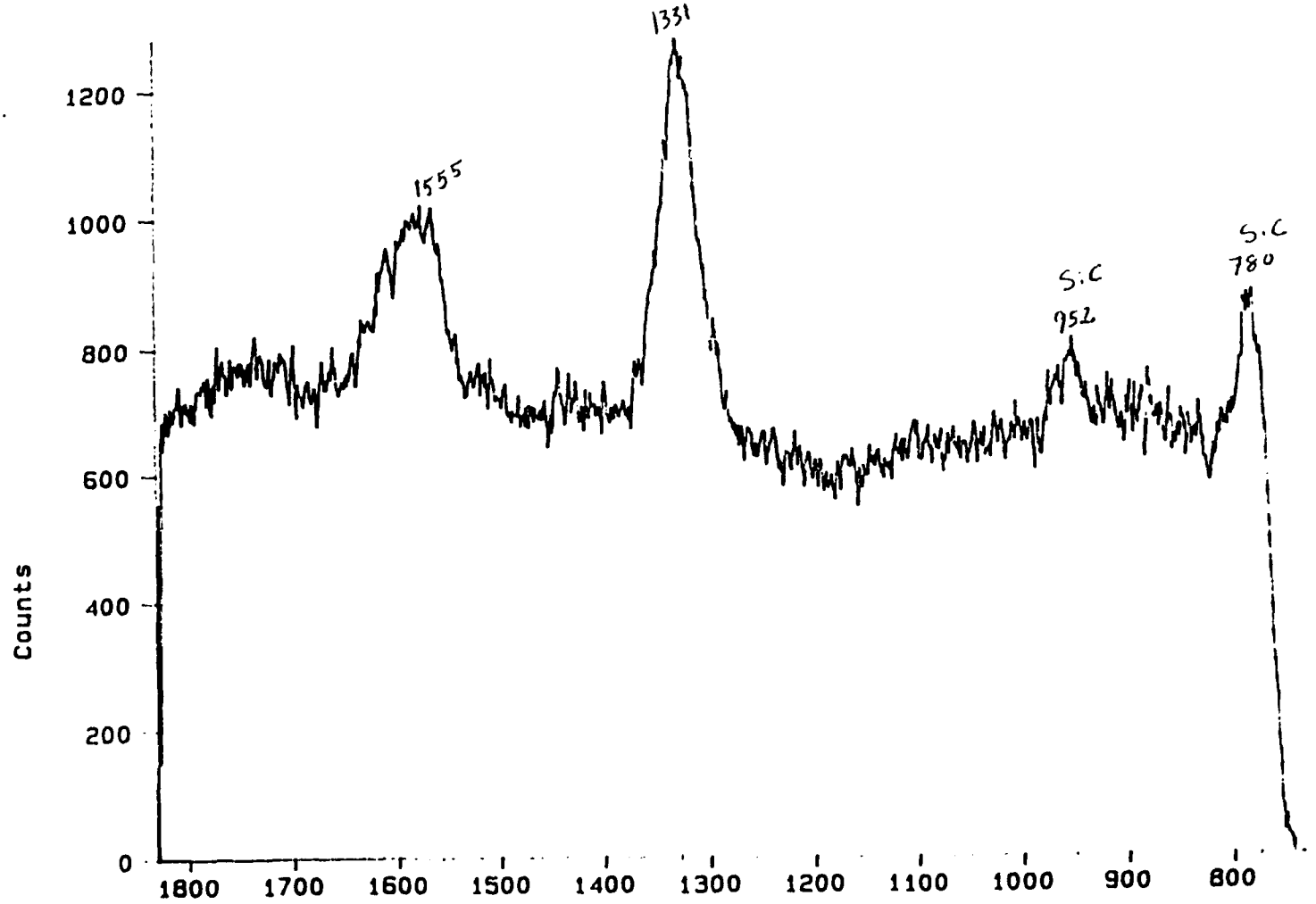

Figure 12. Raman spectrum of Sample # 57 showing diamond and DLC peaks in addition to SiC peaks

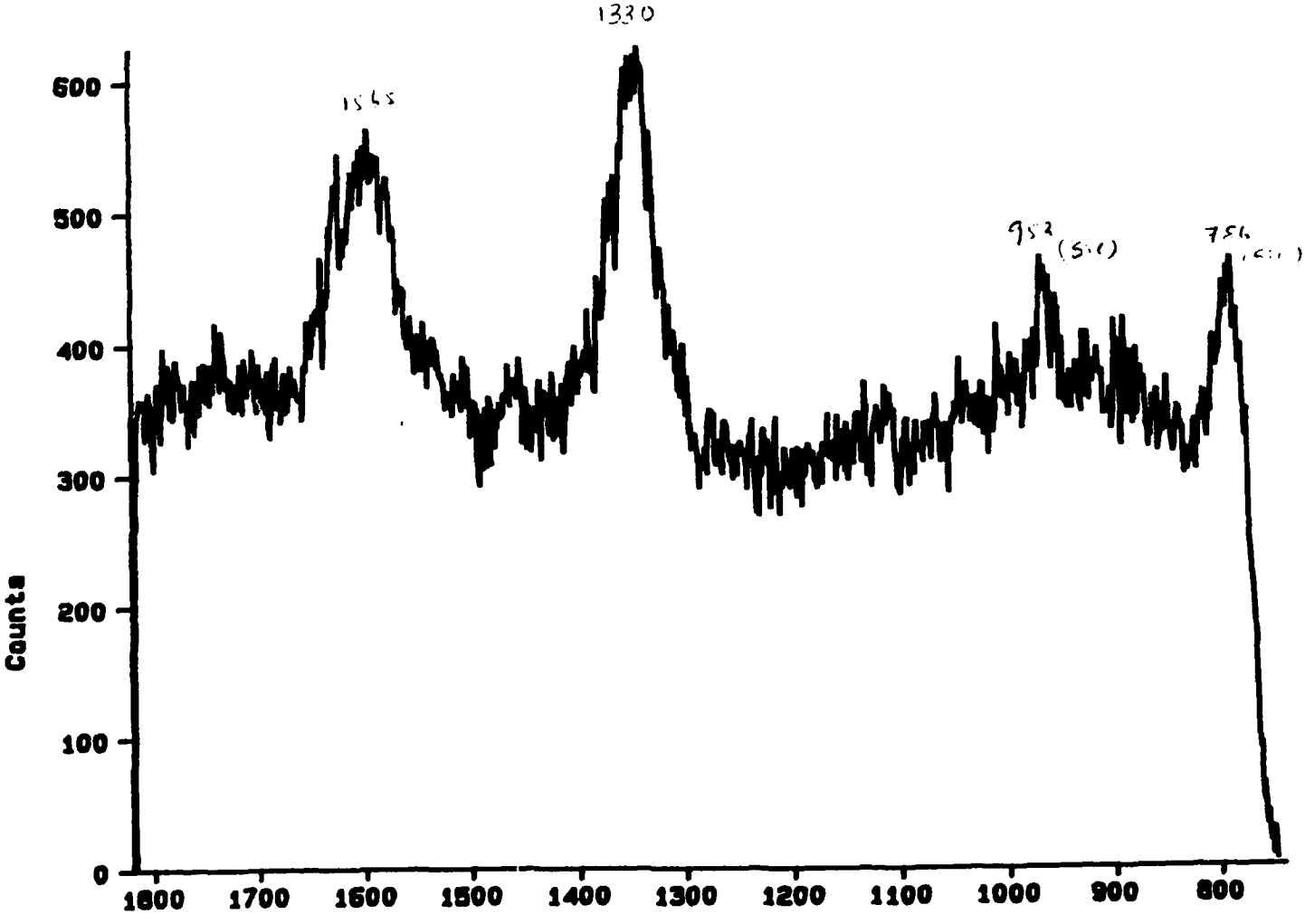

Figure 13. Raman spectrum of Sample # 58 showing diamond and DLC peaks in addition to SiC peaks

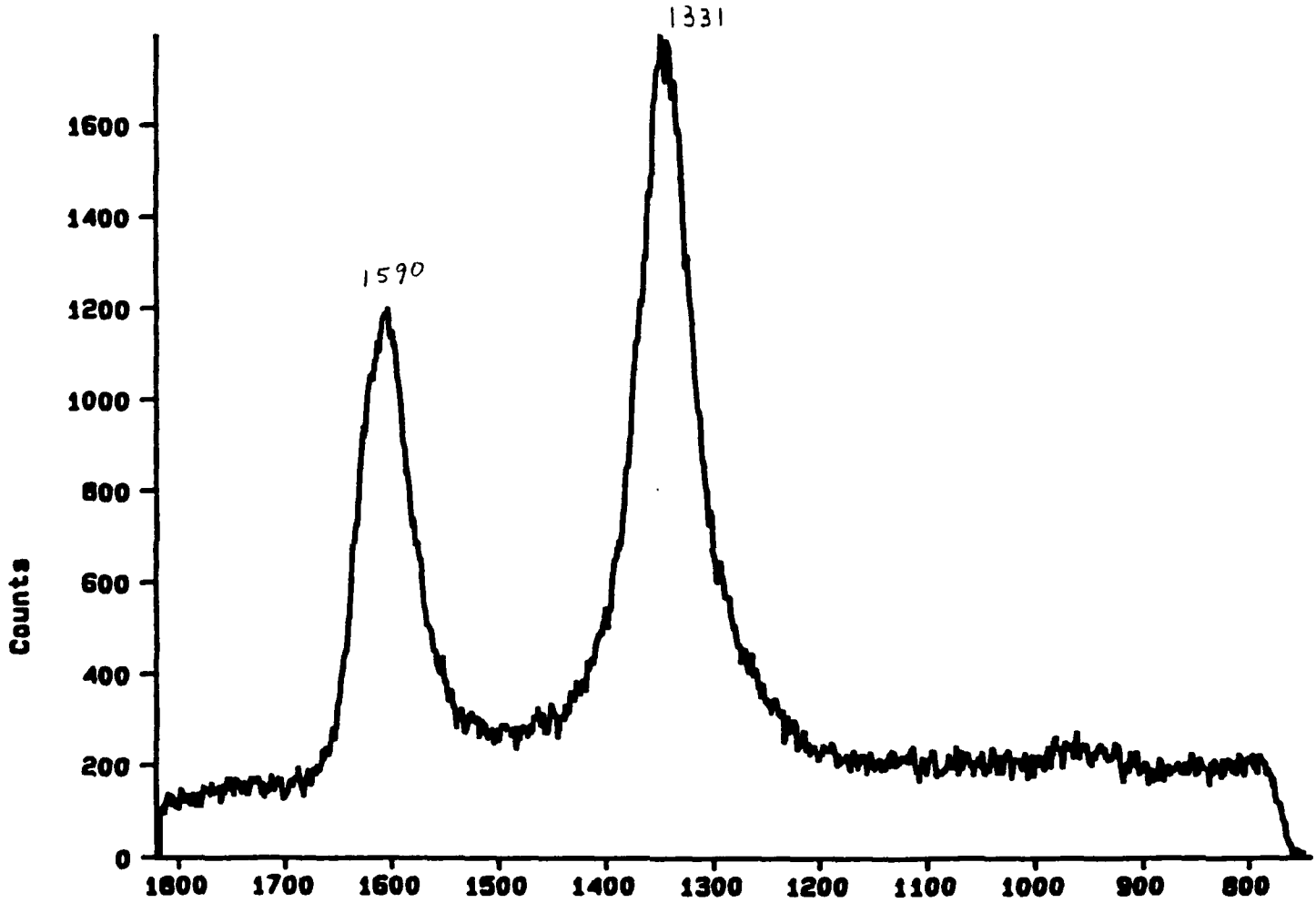

Figure 14. Raman spectrum of Sample # 64 showing diamond and DLC peaks
Note the absence of SiC peaks

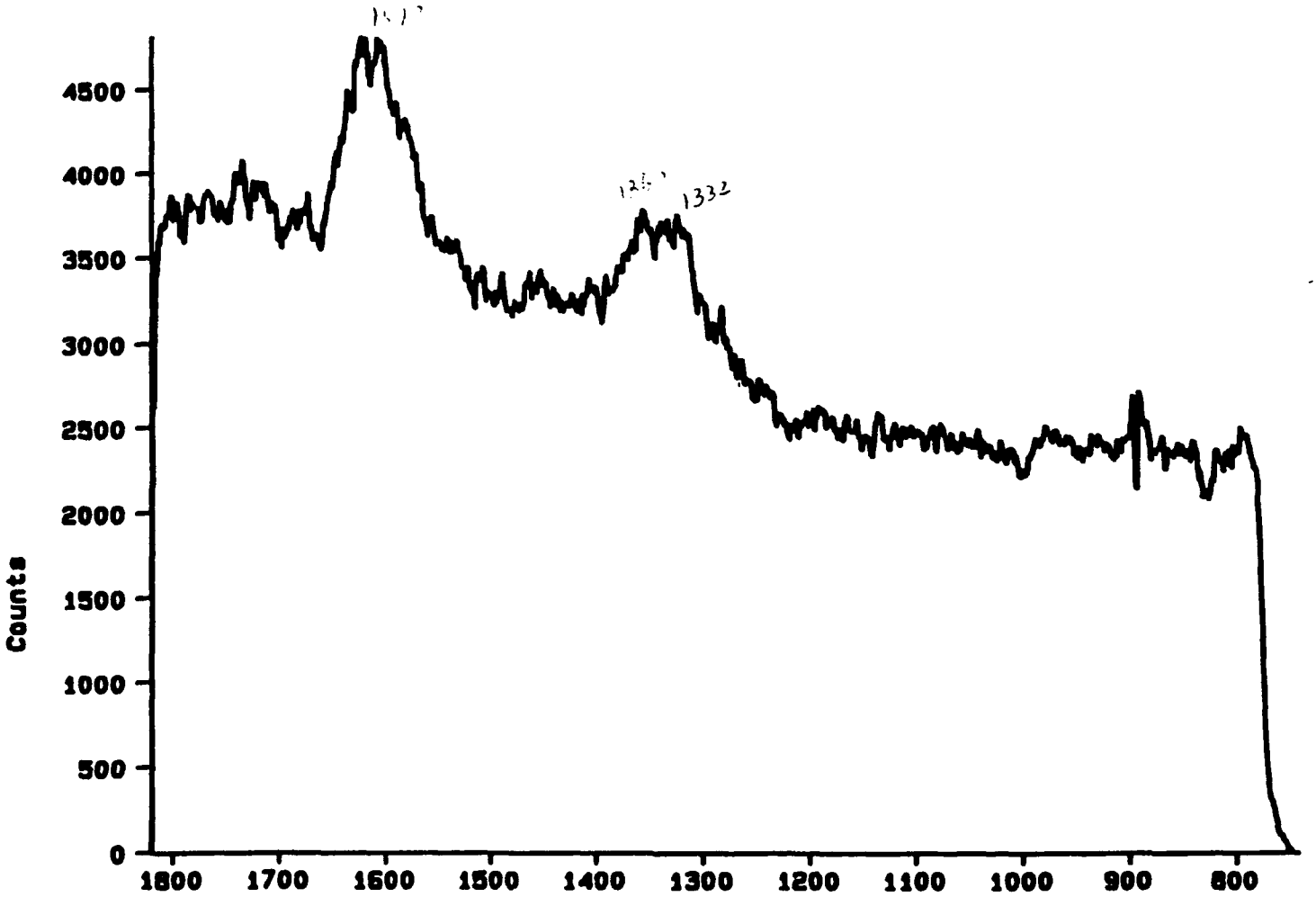

Figure 15. Raman spectrum of Sample # 65 showing diamond and DLC peaks Note the absence of SiC peaks

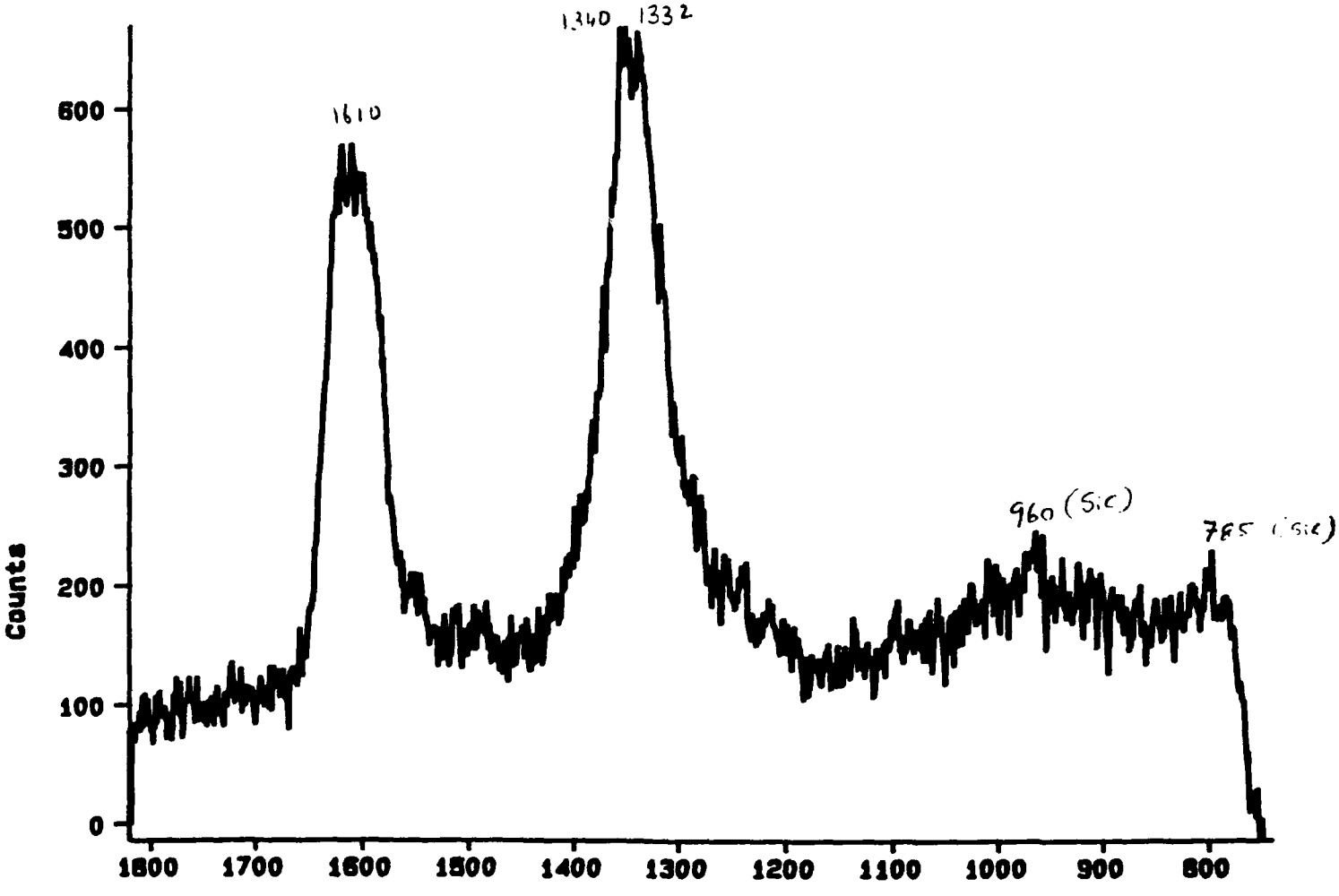

Figure 16. Raman spectrum of Sample # 73 showing diamond and DLC peaks in addition to SiC peaks

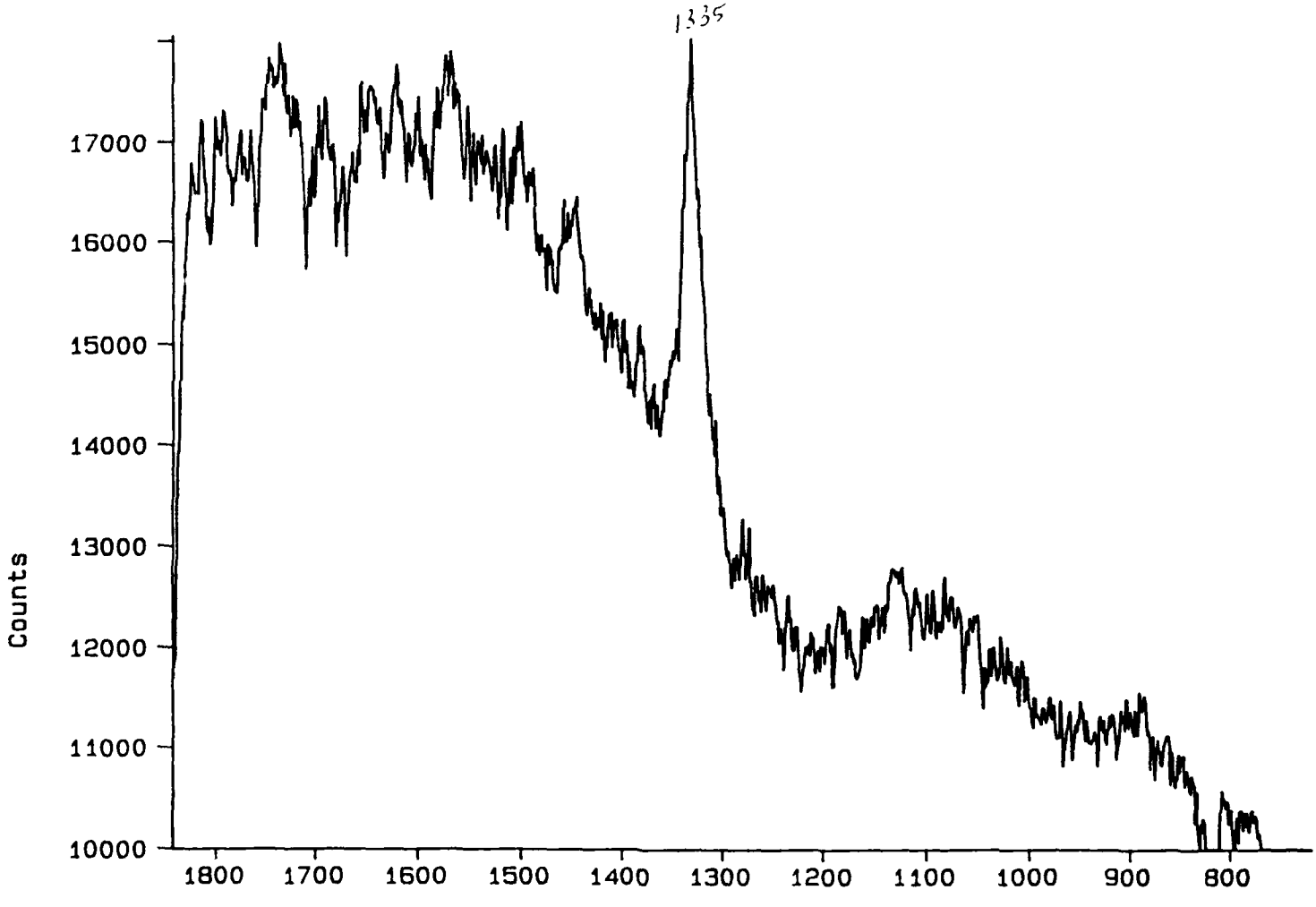

Figure 17. Raman spectrum of hot-filament CVD grown diamond film on Si

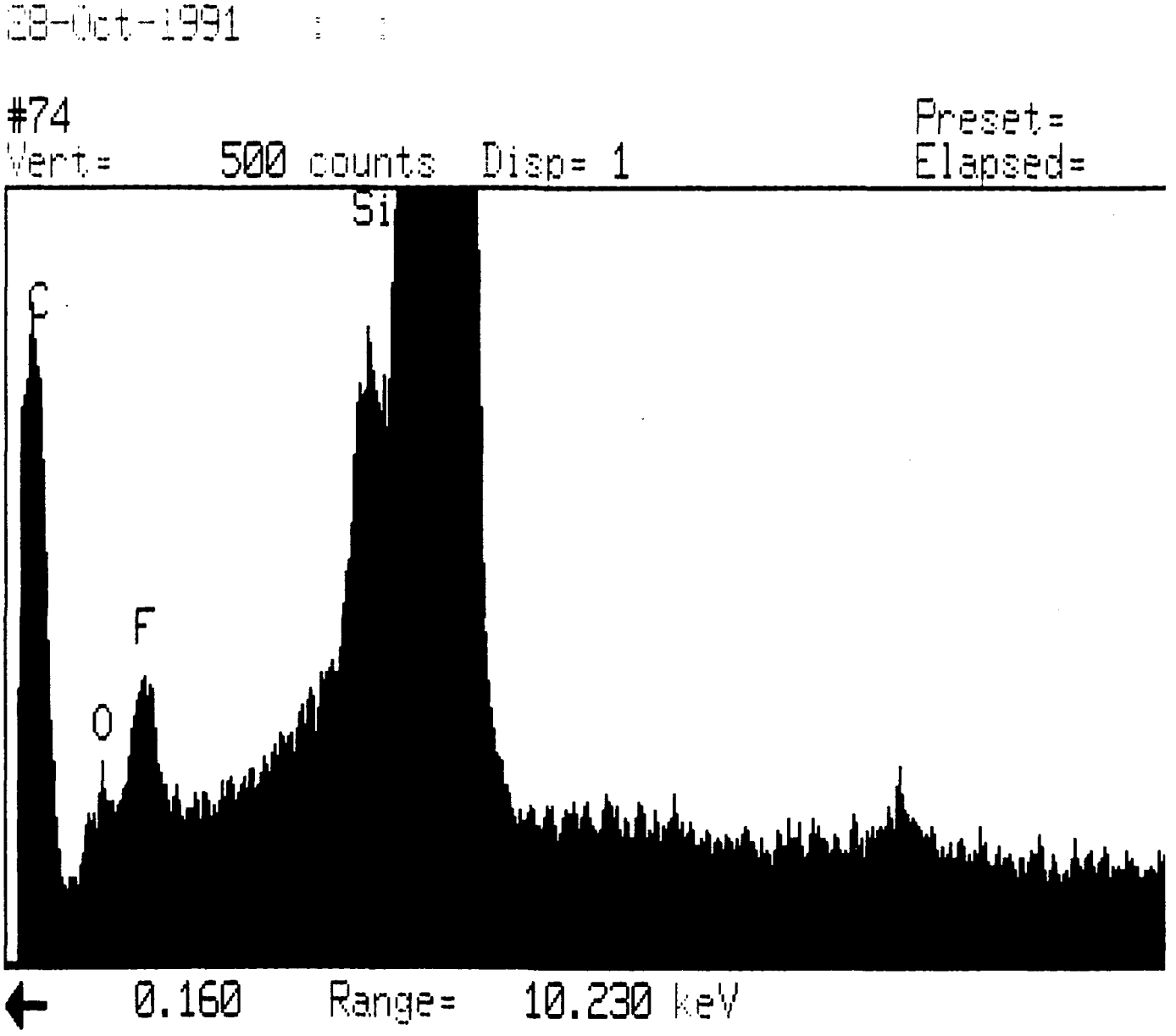

Figure 18. Wavelength dispersive X-ray spectrum of Sample # 74 showing carbon and fluorine

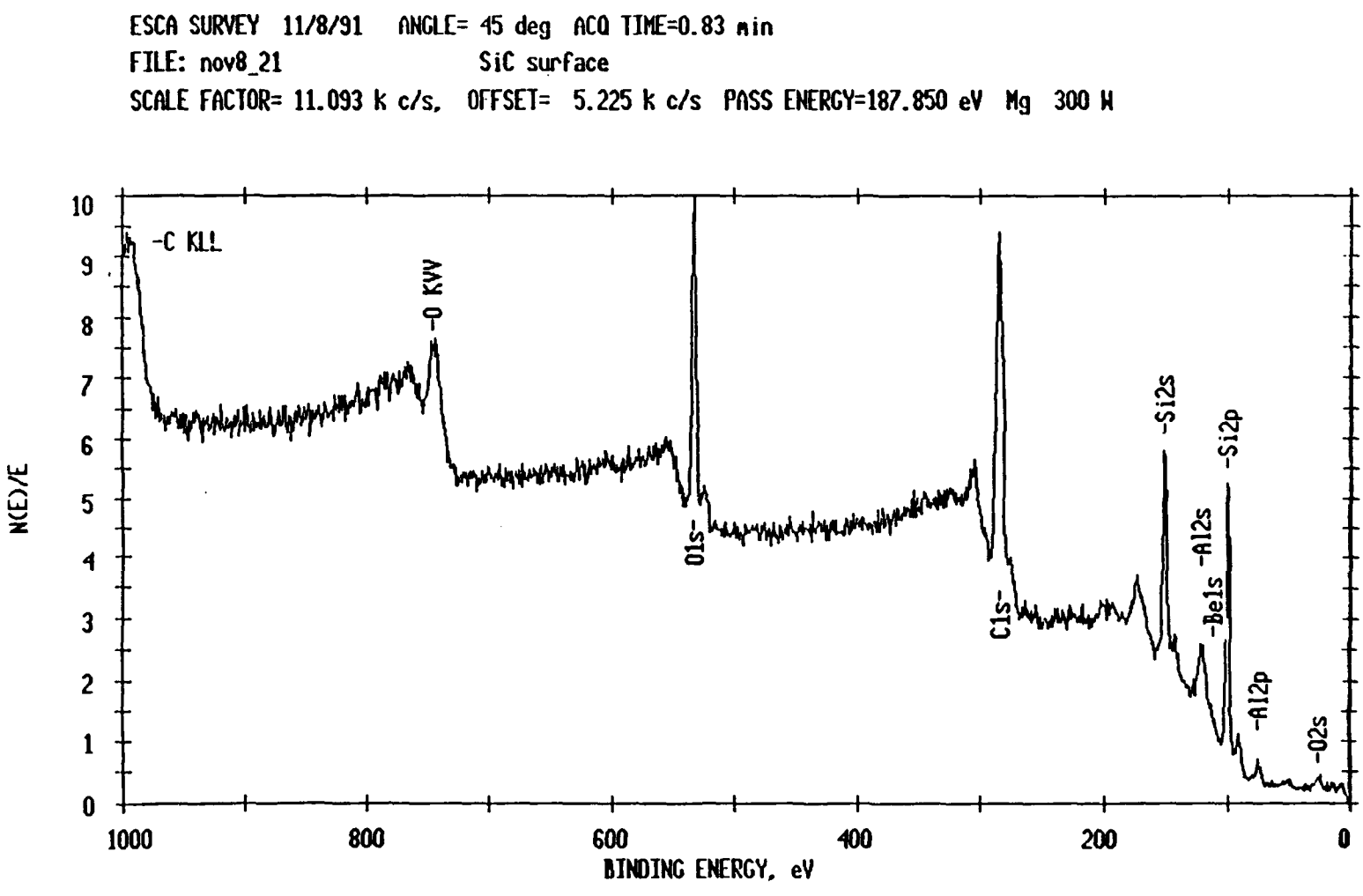

Figure 19. Full scale XPS spectrum of SiC substrate

ESCA SURVEY 11/8/91 ANGLE= 45 deg ACQ TIME=1.25 min
FILE: nov8_6 Laser modified SiC surface
SCALE FACTOR= 11.128 k c/s, OFFSET= 0.967 k c/s PASS ENERGY=187.850 eV Mg 300 W

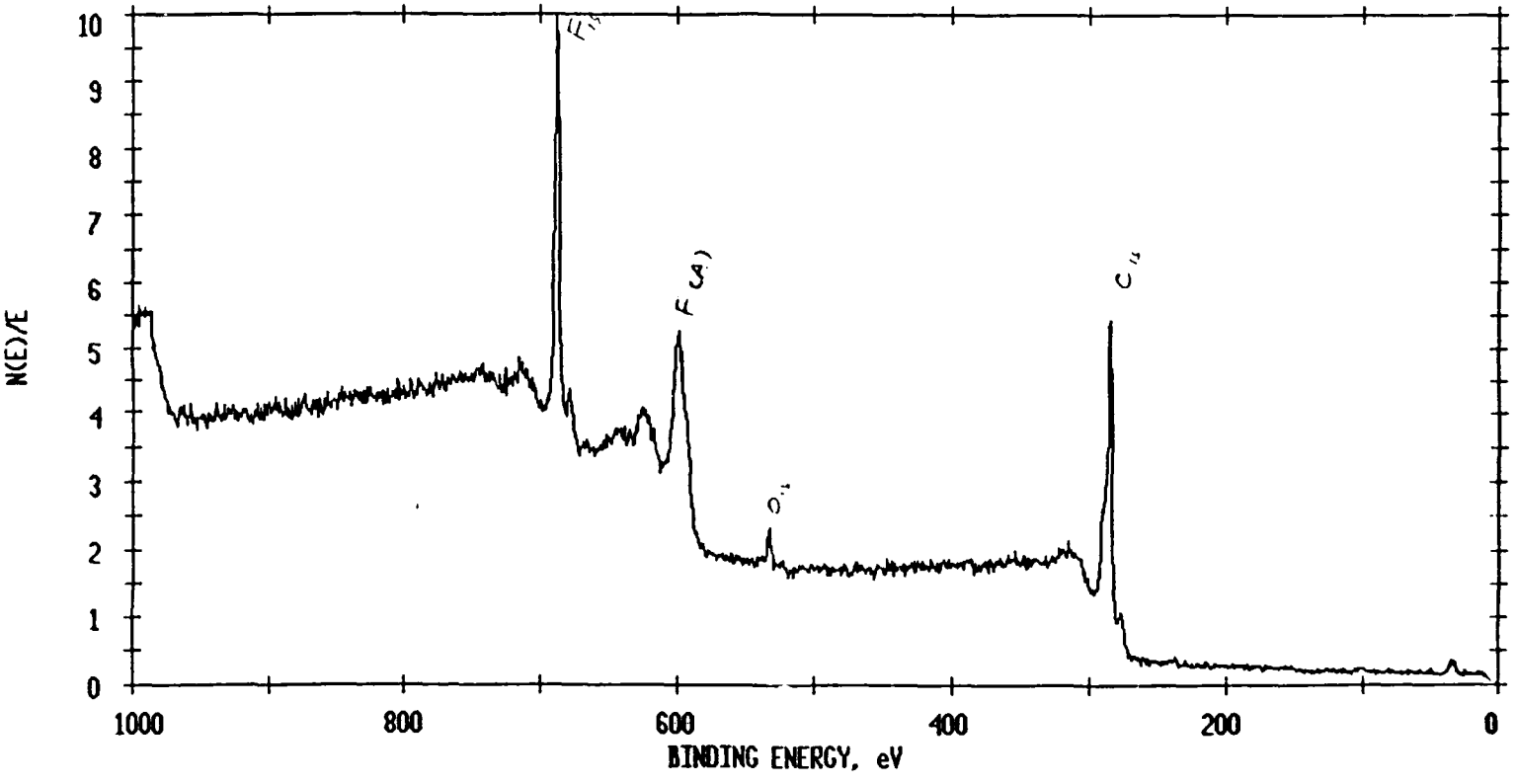

Figure 20. Full scale XPS spectrum of Sample # 64

ESCA SURVEY 11/8/91 ANGLE= 45 deg ACQ TIME=1.67 min
FILE: nov8_3 Laser modified SiC surface
SCALE FACTOR= 9.761 k c/s, OFFSET= 0.863 k c/s PASS ENERGY=187.850 eV Mg 300 W

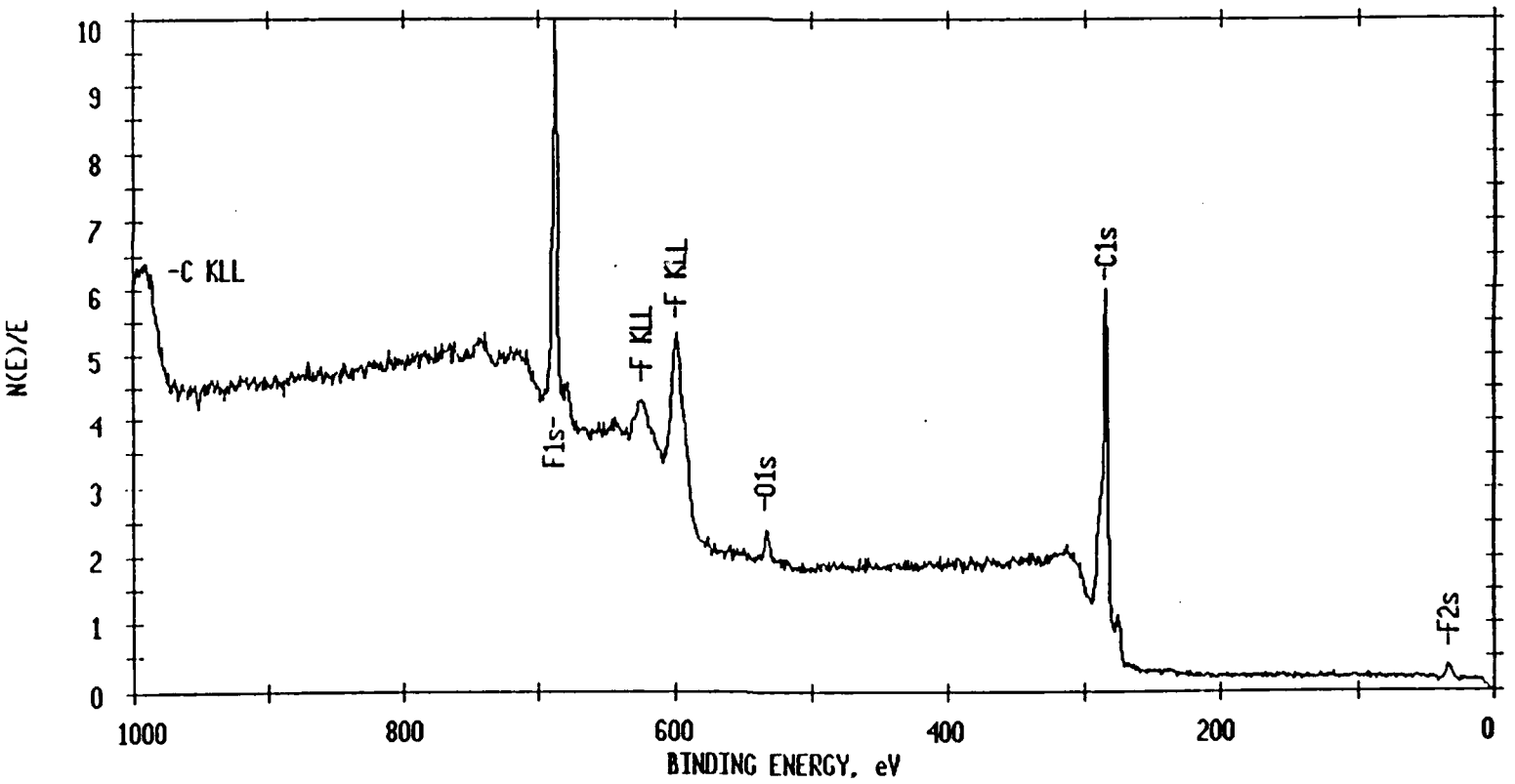

Figure 21. Full scale XPS spectrum of Sample # 74

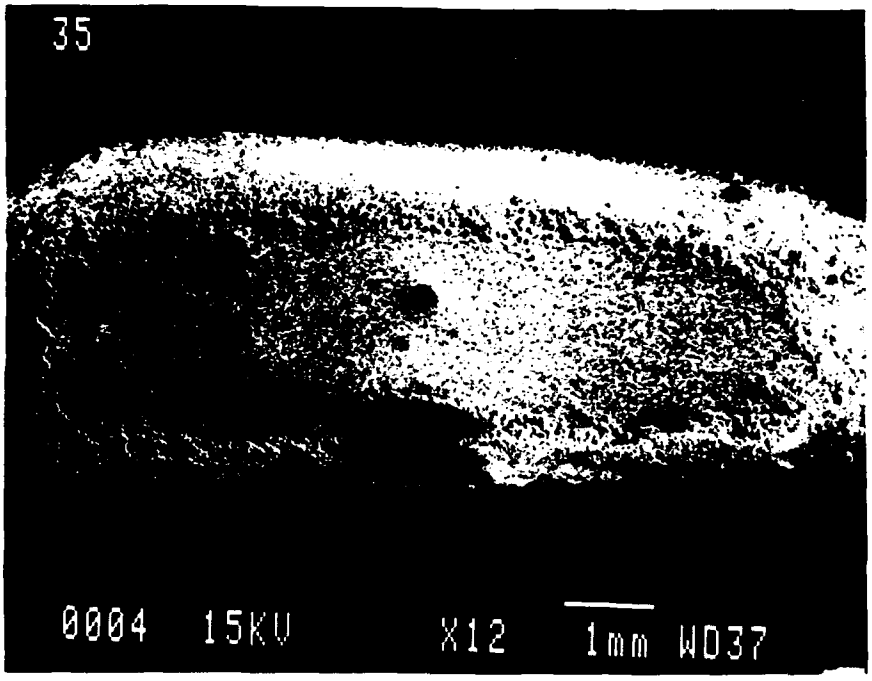

Figure 22. Scanning electron micrograph of laser grown film on 440C stainless steel. The dark zone is a beam-masked area intended to determine the thickness of film

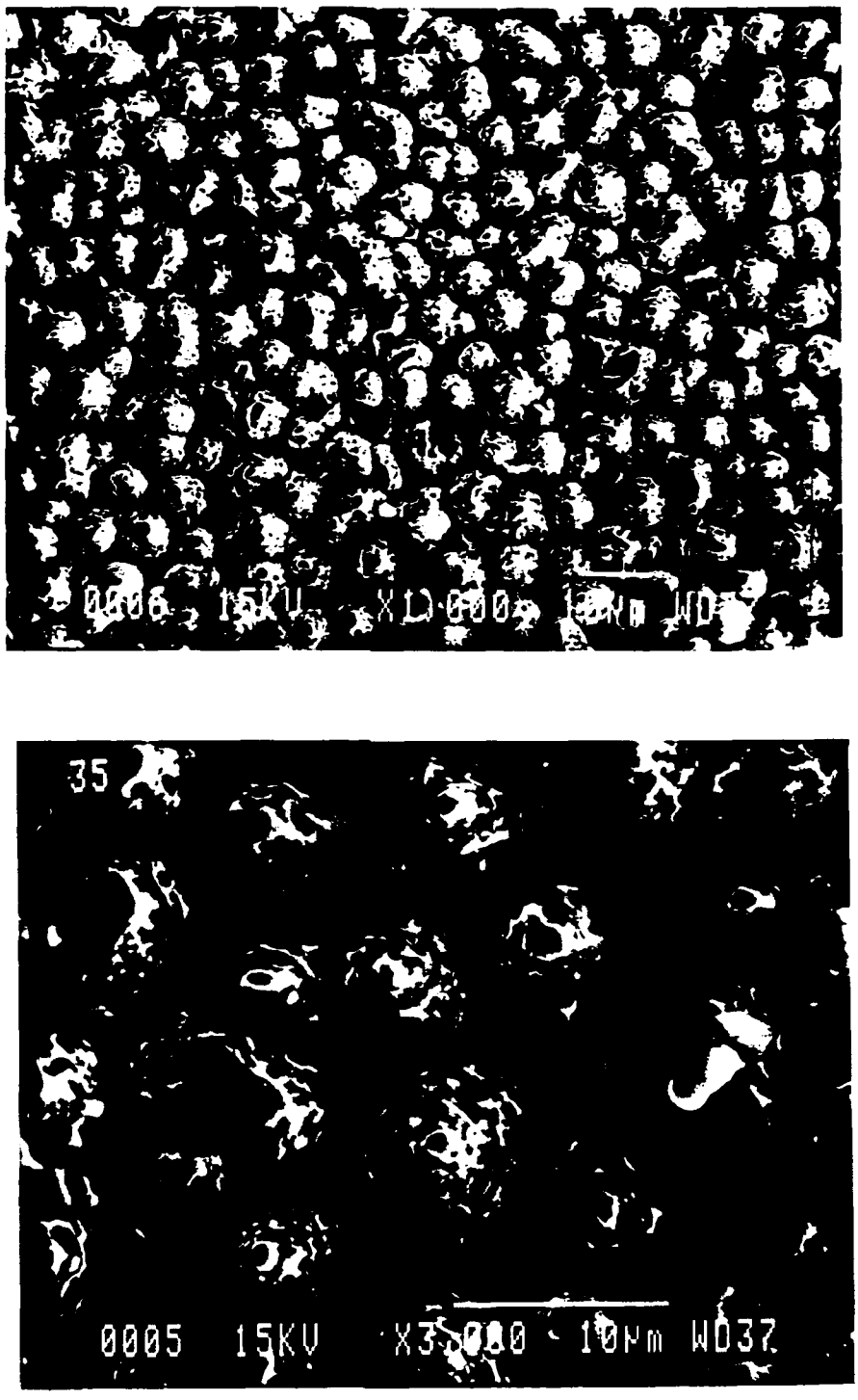

Figure 23. Scanning electron micrographs of Sample # 35 showing ball-like diamond structures

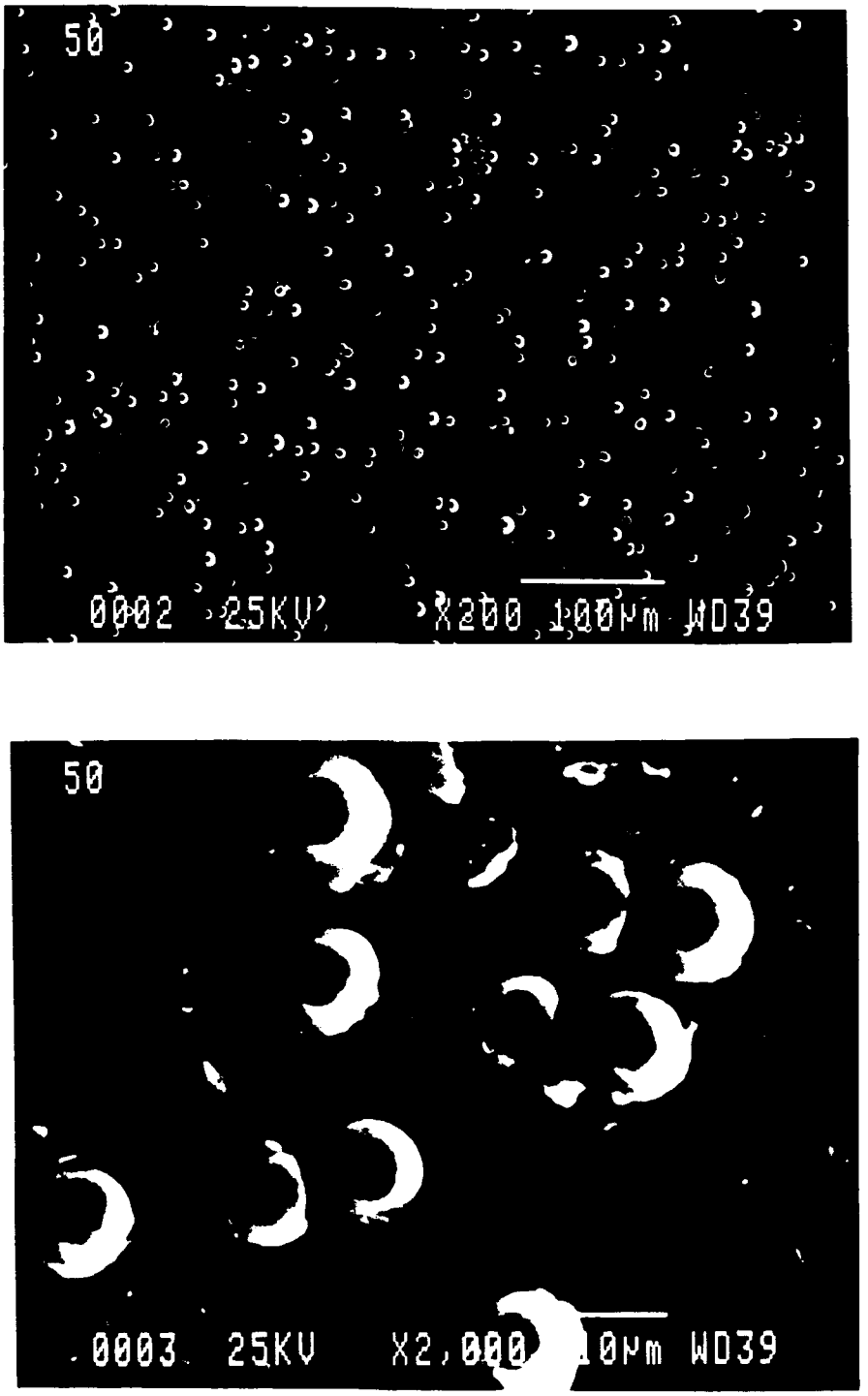

Figure 24. Scanning electron micrographs of Sample # 50 showing mixed carbon structures

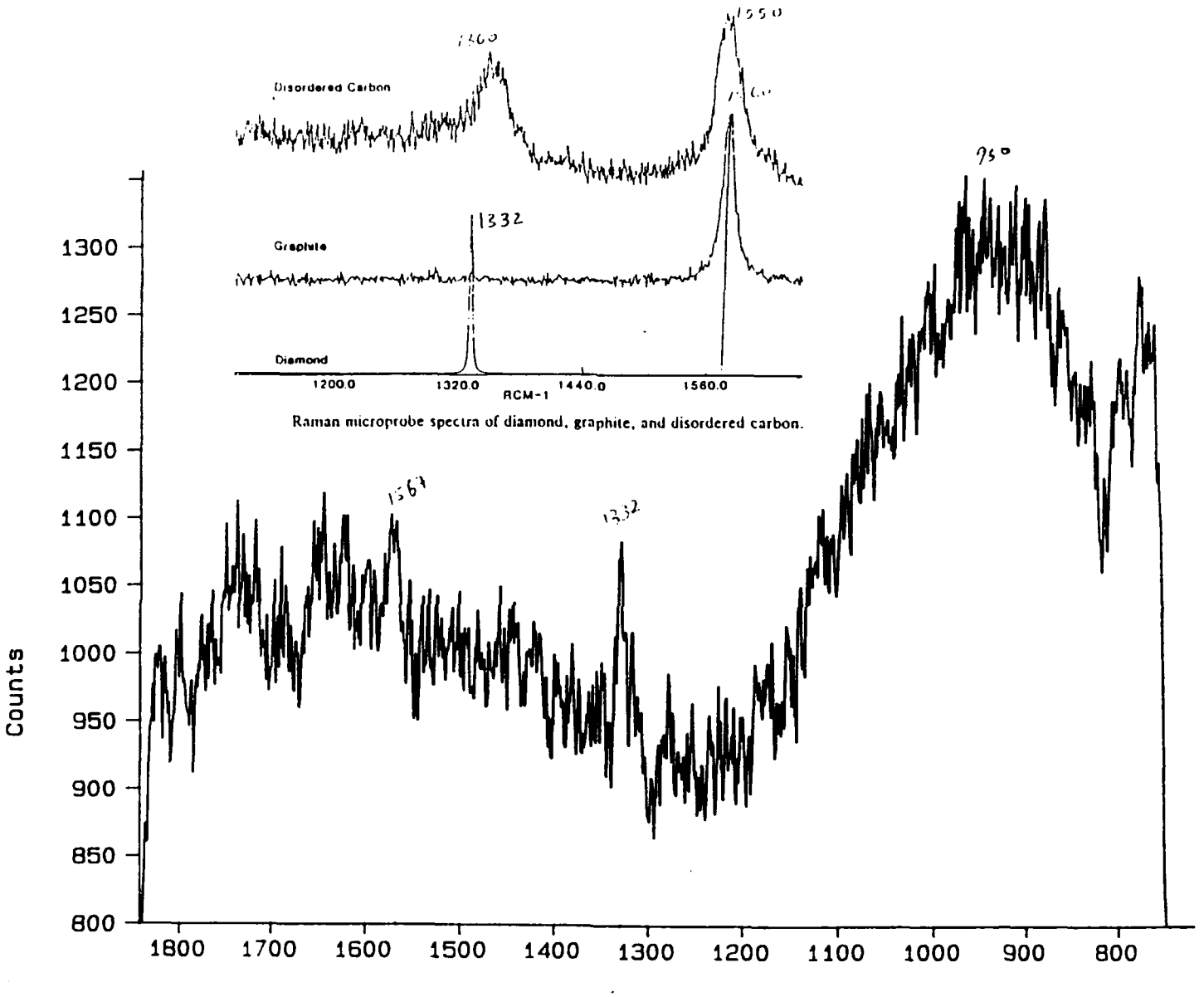

Figure 25. Raman spectrum of Sample # 35 showing diamond and DLC

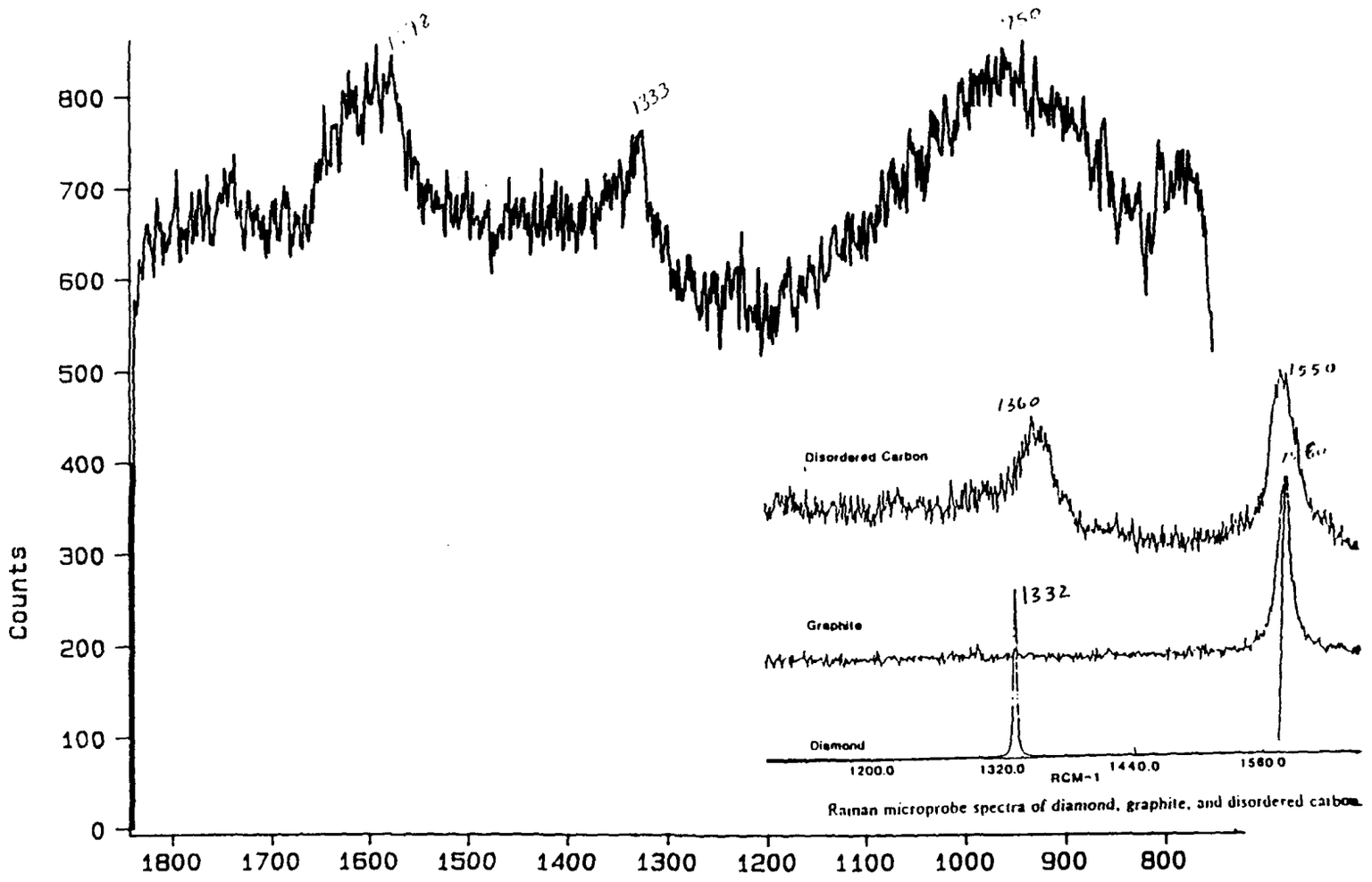

Figure 26. Raman spectrum of Sample # 38 showing diamond and graphite

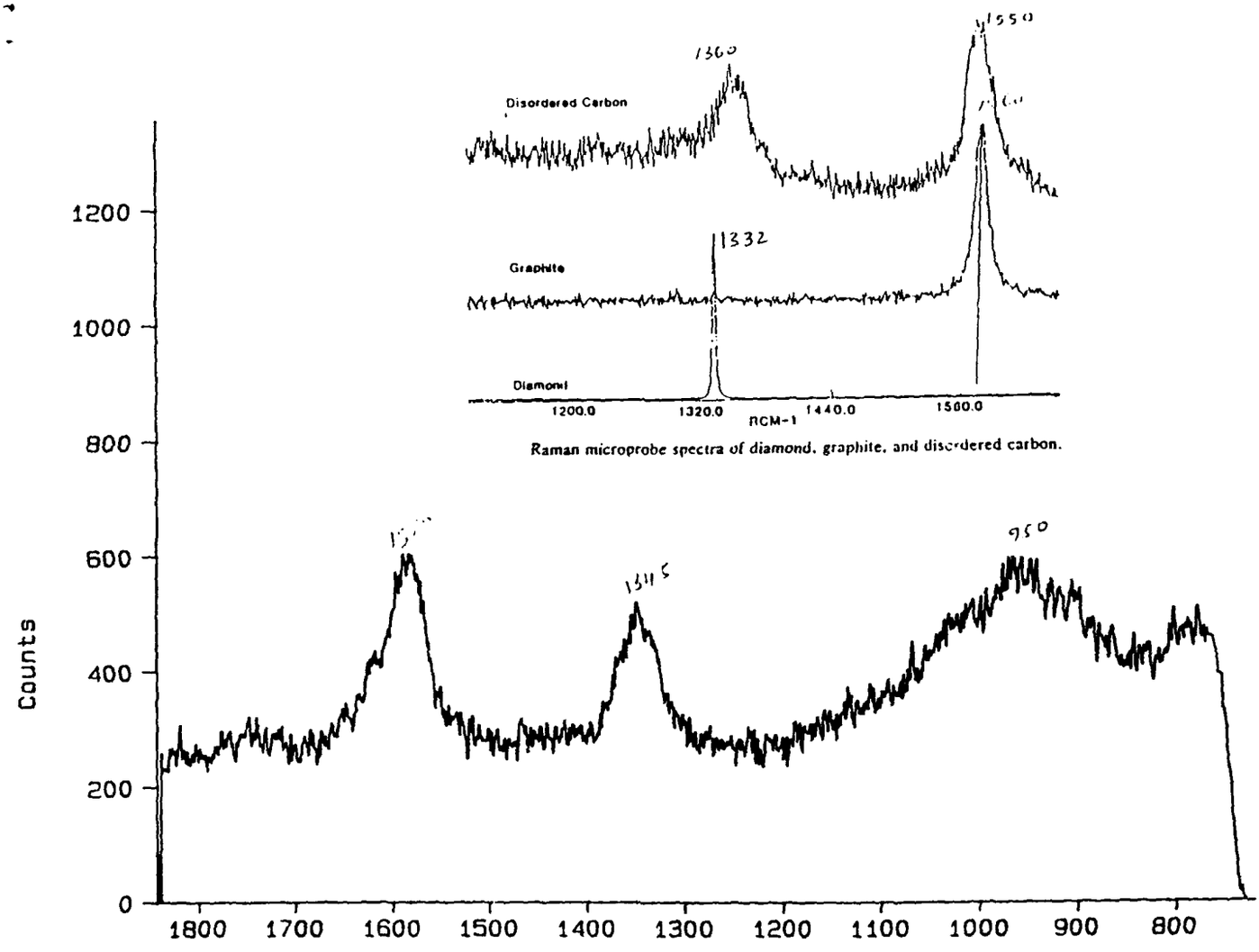

Figure 27. Raman spectrum of Sample # 40 showing DLC and graphite

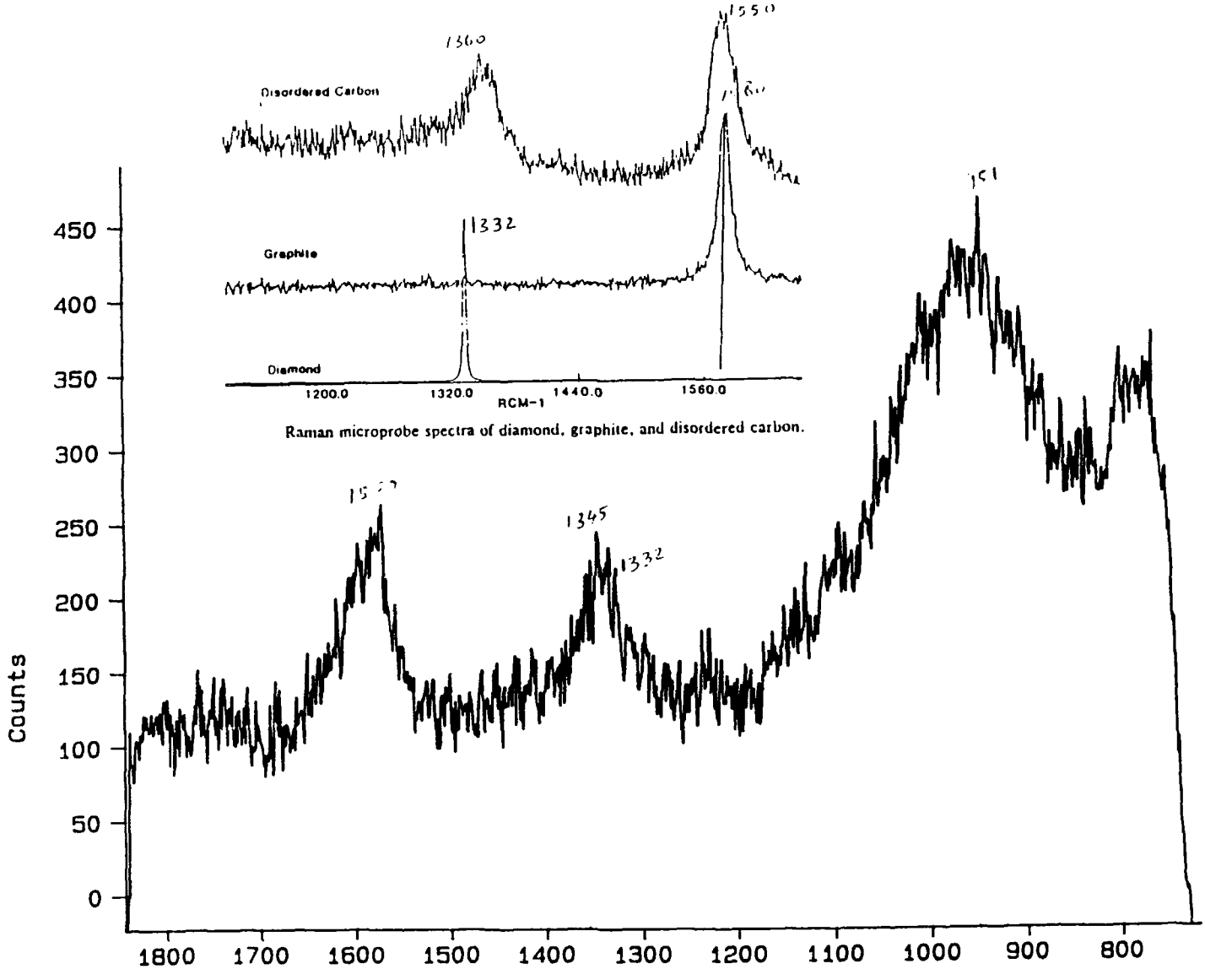

Figure 28. Raman spectrum of Sample # 46 showing diamond, DLC and graphite

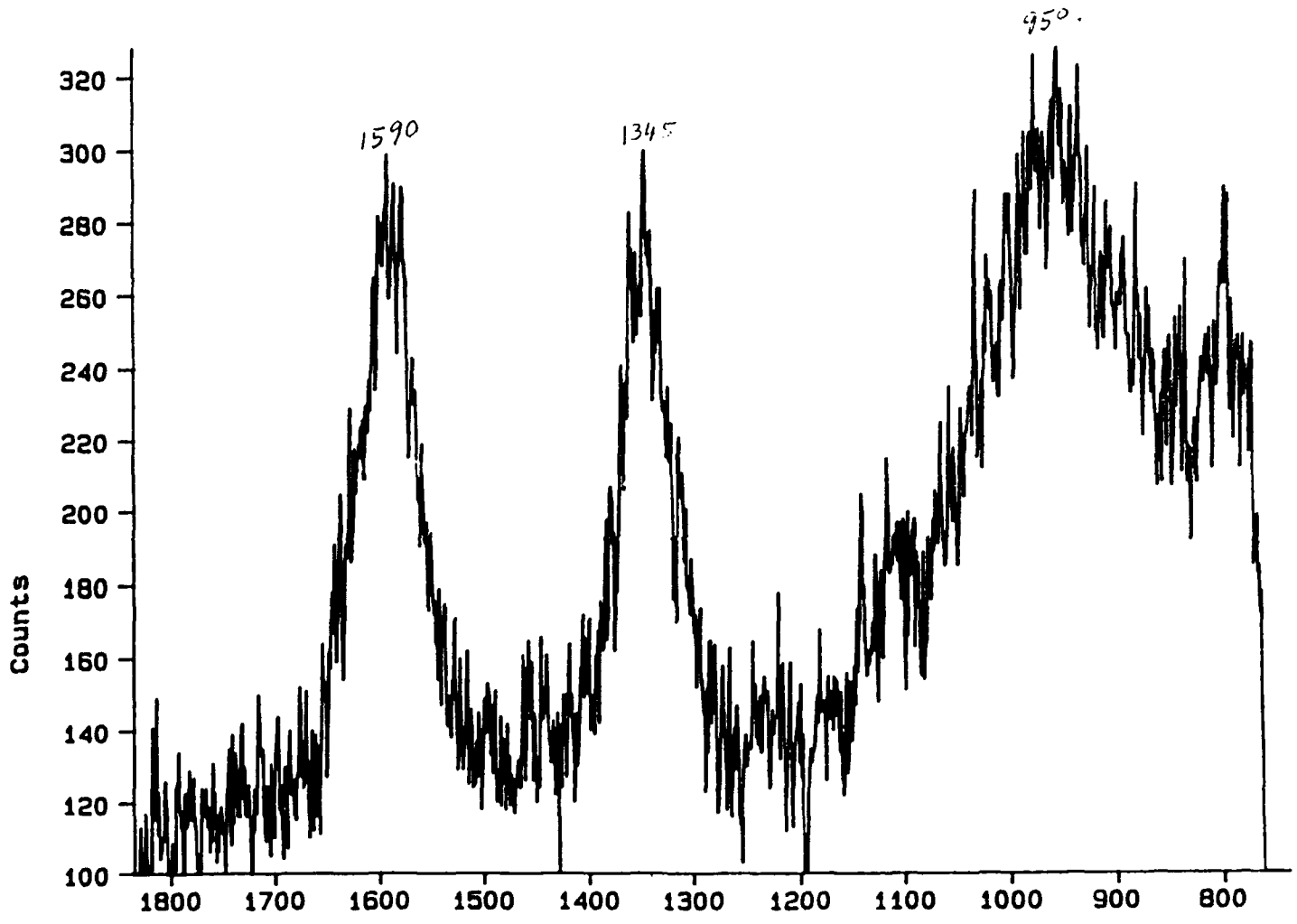

Figure 29. Raman spectrum of Sample # 50 showing DLC and graphite

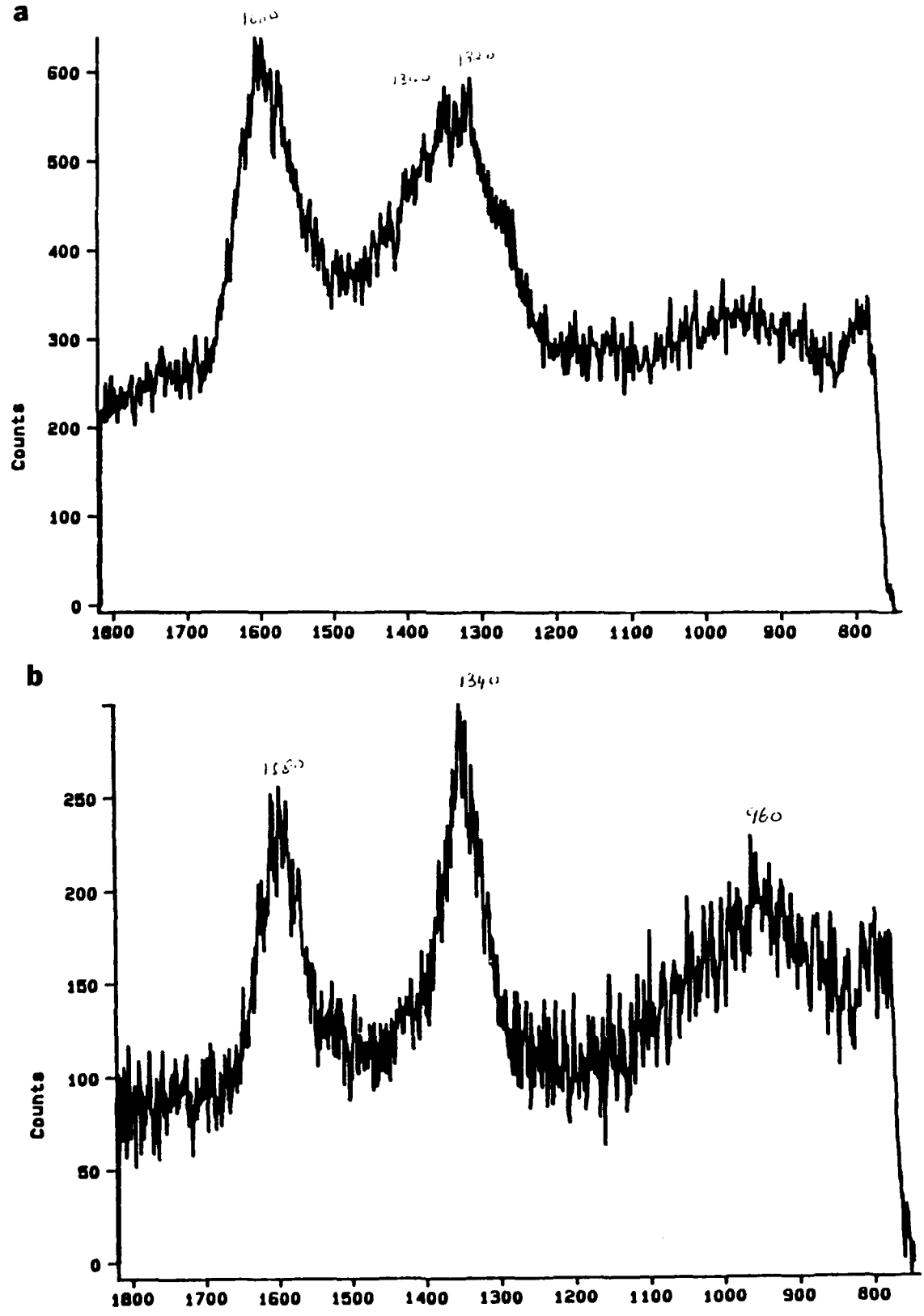

Figure 30. Effect of beam wavelength on Raman spectrum of diamond films
(a) 193-nm ArF beam processed
(b) 248-nm KrF beam processed

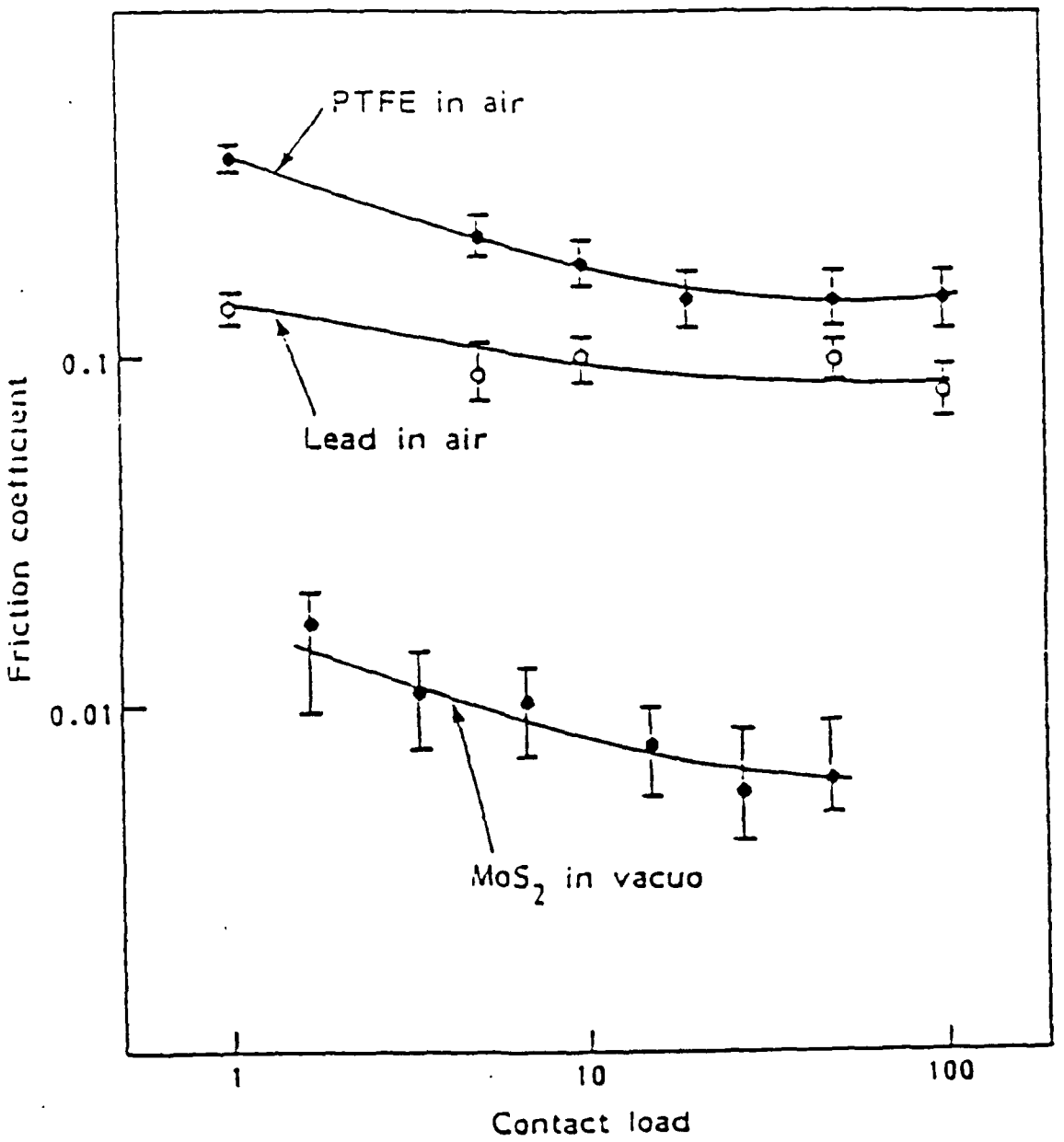

Figure 31. Friction data of three commonly employed space lubricants on steel substrates

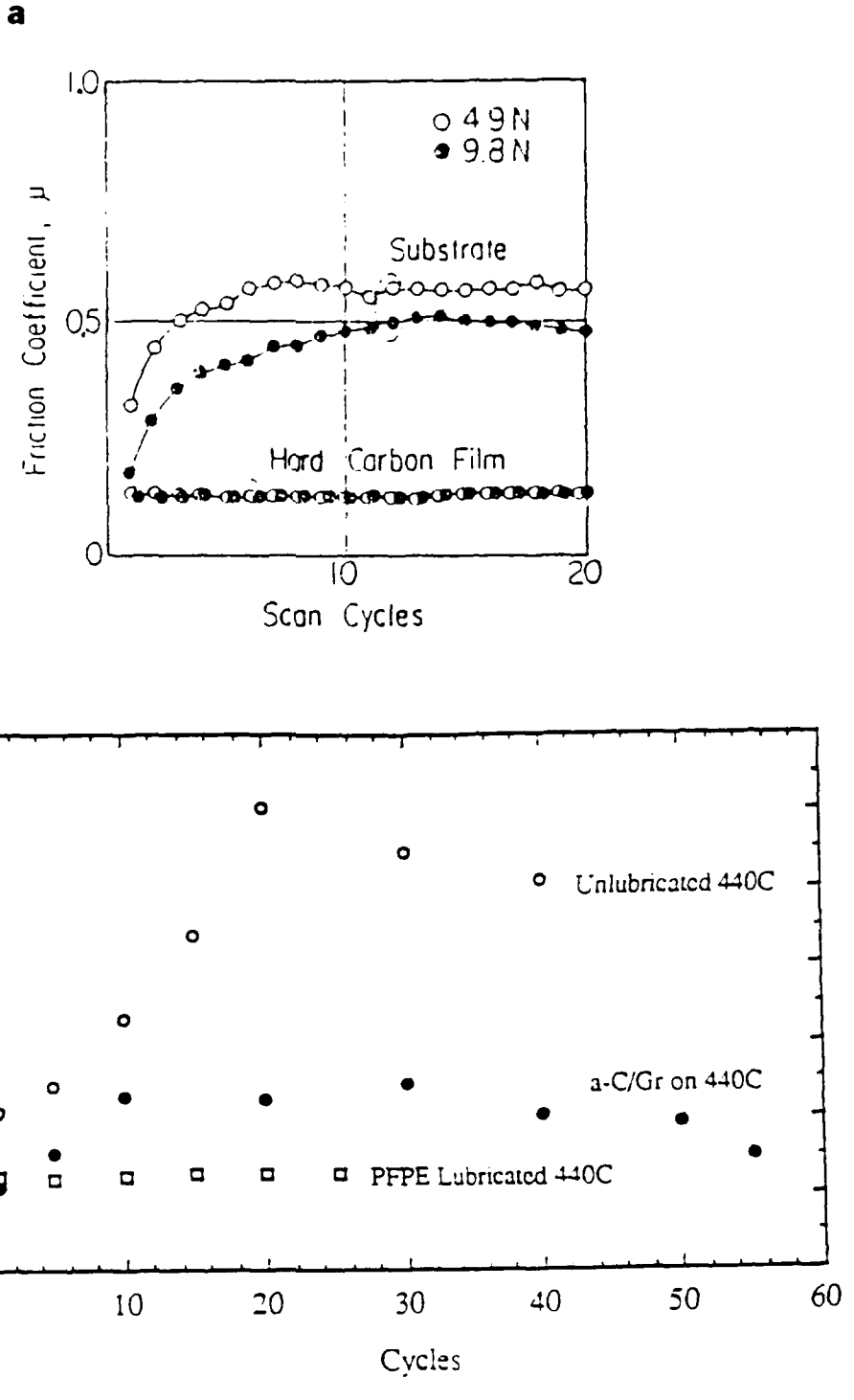

Figure 32. Friction of hard carbon films on 440C steel
(a) From Reference 7
(b) From Reference 8